The transcription factor ESR2/DRNL/BOL orchestrates cytokinin dynamics leading to developmental reprogramming and green callus formation

Yolanda Durán-Medina[1], David Díaz-Ramírez[1], Humberto Herrera-Ubaldo[2], Maurizio Di Marzo[3], J. Erik Cruz-Valderrama[2], Herenia Guerrero-Largo[1], Beatriz E. Ruiz-Cortés[1], Andrea Gómez Felipe[2], J. Irepan Reyes-Olalde[2], Lucia Colombo[3], Ondrej Novak[4], Stefan de Folter[2], Nayelli Marsch-Martínez[1]

[1]Biotechnology and Biochemistry department, Irapuato Unit, Cinvestav, Mexico

[2]Advanced Genomics Unit (UGA), Cinvestav, Irapuato, Mexico

[3]Department of Biosciences, University of Milan, Milan, Italy

[4]Laboratory of Growth Regulators, Centre of the Region Haná for Biotechnological and Agricultural Research, Institute of Experimental Botany, Czech Academy of Sciences, and Faculty of Science, Palacký University, Czechia

Corresponding author: Nayelli Marsch-Martinez (Nayelli.marsch@cinvestav.mx)

Short title: ESR2 and cytokinin dynamics in callus formation

The author responsible for distribution of materials integral to the findings presented in this article in accordance with the policy described in the Instructions for Authors (https://academic.oup.com/plphys/pages/General-Instructions) is Nayelli Marsch Martínez.

Abstract

Callus formation and shoot regeneration are naturally triggered by stress and damage to the plant. They are also key components of tissue culture, which is crucial for gene editing, transformation, propagation, and other technologies in many species. Thus, the study of callus formation and shoot regeneration provides valuable insights into plant development. The transcription factor ENHANCER OF SHOOT REGENERATION 2 / DORNROSCHEN-LIKE / BOLITA / SUPPRESSOR OF PHYTOCHROME B-4 2 (ESR2/DRNL/BOL/SOB2) promotes green callus formation in roots as well as shoot regeneration when overactive, and the phythormone cytokinin plays a prominent role in both processes. Yet, the role of ESR2 in the cytokinin pathway has not been previously described in Arabidopsis (*Arabidopsis thaliana*). We found that cytokinin content and the expression of the cytokinin biosynthesis gene *ISOPENTENYLTRANSFERASE 5* (*IPT5*) are greater in plants with high ESR2 activity. ESR2 also regulates the cytokinin signaling repressor *ARABIDOPSIS HISTIDINE PHOSPHOTRANSFER PROTEIN 6* (*AHP6*), and surprisingly, ESR2-stimulated green callus formation requires *IPT5* and *AHP6*. Therefore, ESR2 promotes both cytokinin biosynthesis and the inhibition of cytokinin signaling and, paradoxically, requires

a combination of these two effects for green callus induction. These findings provide a foundation to better understand the processes involved in tissue reprogramming towards callus formation and the role of ESR2 in callus formation and shoot regeneration.

INTRODUCTION

The remarkable regenerative capacity of plants allows the emergence of new organs or complete plants from a small piece of somatic tissue. This capacity highlights the incredible plasticity of plant cells, which has long attracted the interest of researchers (Gordon et al., 2007; Ibáñez et al., 2020; Ikeuchi et al., 2016). Great advance in the study of plant cellular plasticity occurred after the discovery of the phytohormones auxin and cytokinin and their application to *in vitro* plant tissue culture (Melnyk, 2023). The auxin/cytokinin phytohormone ratio is key for the fate specification of plant cells. In 1957, Skoog and Miller's pioneering work using tobacco (*N. tabacum*) explants revealed that high ratios of auxin-to-cytokinin or cytokinin-to-auxin induce root or shoot regeneration, respectively, while an intermediate ratio of auxin and cytokinin promotes a mass of growing cells known as "callus" (Skoog & Miller, 1957; Melnyk, 2023). Since then, callus has been widely used as a valuable tool for the propagation and genetic engineering of a wide variety of plants, and other biotechnological applications (Ikeuchi et al., 2013; Efferth, 2019). This type of tissue benefits from indefinite growth while it is maintained in a callus-inducing medium, but when it is moved to a new medium with the right combination of cytokinin and auxin, it is possible to obtain shoot or root regeneration (Skoog & Miller, 1957). Recent research has advanced the understanding of the molecular mechanisms underlying cytokinin's function in the control of green callus formation and shoot regeneration (reviewed in Šmeringai et al., 2023).

ENHANCER OF SHOOT REGENERATION (ESR) transcription factors can also trigger callus and shoot formation. They belong to the APETALA2/Ethylene Response Factor (AP2/ERF) superfamily. The overexpression of *ESR1/DORNRÖSCHEN (DRN)* in Arabidopsis promotes cytokinin-independent shoot generation and increases shoot regeneration efficiency in the presence of cytokinin (Banno et al., 2001). *ESR2/BOLITA (BOL)* overexpression or gain of function also induces callus and shoot production without exogenous phytohormone application, and it is more active than ESR1 in promoting shoot regeneration in tissue culture (Ikeda et al., 2006; Marsch-Martinez et al., 2006). Accordingly, the loss of *ESR2* function impairs shoot regeneration at a greater extent than the loss of *ESR1* (Matsuo et al., 2011). Curiously, calli induced by ESR2 are green (Marsch-Martinez et al., 2006), and recently, chlorenchyma (green) cells in

calli have been found to play a crucial role in shoot regeneration (Song et al., 2023). ESR2 is also known as DORNRÖSCHEN-LIKE (DRNL) (Chandler & Werr, 2014; Kirch et al., 2003) and SUPPRESSOR OF PHYTOCHROME B-4 2 (SOB2) (Ward et al., 2006). In this work, focused on callus development, it will be referred to as ESR2. The *ESR2* expression pattern precedes and partially overlaps local auxin maxima, as revealed by the synthetic auxin response reporter DR5 (Chandler et al., 2011; Chandler & Werr, 2014), and ESR2 indirectly regulates auxin biosynthesis through the transcription factor STYLISH1 (STY1) (Eklund et al., 2011). However, the effects of increased ESR2 expression closely resemble the effects of increased cytokinin levels, such as the dark green color in leaves (Cortleven & Schmülling, 2015), primary root growth inhibition (Dello Ioio et al., 2007; Liu et al., 2022; Werner et al., 2003), and green callus development (Ikeuchi et al., 2013; Sakai et al., 2001). The ESR2 induction phenotype has been described as comparable to the phenotype of mutants overproducing cytokinins (Ikeda et al., 2006). ESR2 overexpression also affects the expression of genes related to the cytokinin pathway (Ikeda et al., 2006a; Marsch-Martinez et al., 2006). Our previous research on gynoecium development indicated a positive regulatory effect of ESR2 on the cytokinin pathway at the early stages of gynoecium development (Durán-Medina et al., 2017a). Furthermore, the mutation of the single tomato homolog of *ESR1* and *ESR2*, *LEAFLESS (LFS)*, alters the expression of cytokinin biosynthesis and signaling genes, suggesting a positive regulatory role (Capua & Eshed, 2017). Therefore, based on this data, this study aimed to investigate the role of ESR2 as a positive regulator of the cytokinin pathway (biosynthesis or signaling) leading to green callus formation.

RESULTS

ESR2 induction promotes severe defects in seedling organ development

One of the most striking reported effects of *ESR2* is the formation of green calli in roots of young seedlings when the gene is constitutively overexpressed, or in root explants where the overexpression was induced (Ikeda et al., 2006a; Marsch-Martinez et al., 2006). To enhance our understanding about the effects of this transcription factor in plant development, we analyzed the morphological changes in whole seedlings caused by the induction of ESR2 activity after germination in the *35S::ESR2:ER* (*ESR2:ER*) inducible line. In this line, β-estradiol triggers the

entrance of the ESR2 transcription factor into the nucleus, where it regulates gene expression (Eklund et al., 2011; Ikeda et al., 2006). As expected, the induction of ESR2 activity resulted in altered development of aerial and root tissues (Fig. 1A-H). The severity of these morphological alterations depended on the plant developmental stage in which this transcription factor was activated, and the alterations became more evident with the increase in induction time. The induction of ESR2 in seedlings led to an arrest of leaf development (Fig. 1A-D). The induced seedlings did not produce new leaves like those of Wild Type (WT) seedlings, and the leaves that were in early developmental stages at the beginning of the treatment did not expand as non-induced leaves. Moreover, they acquired a dark green color in induced seedlings compared to non-induced ones (Fig. 1A-D). In roots, the developmental changes were also profound. The root apex thickened, coiled, and began to acquire a green color (Fig. 1G-H). The growth of the primary root was arrested, and the induced seedlings had shorter primary roots and a higher number of thick "lateral roots" than non-induced seedlings (Fig 1E). These new thickened lateral roots displayed stunted growth. The induced seedlings had a root length of 37 mm and 8 lateral roots on average, per seedling, while the non-induced seedlings had a root length of 76 mm and 5 lateral roots on average (Fig. 1I-J). In addition, we also observed disorganized lateral root positioning along the main root axis, with some roots growing at an unusual proximity to each other (Fig. 1H). At longer periods of ESR2 induction (21 days), the entire root developed green calli. These green calli developed initially at some distance from each other, at the tip or the base of lateral roots, and subsequently, the whole root became green (Fig. 1F).

In summary, the induction of ESR2 in whole seedlings affected the development of leaves and roots, reducing or inhibiting their growth and leading to green callus development first in regions associated with lateral roots and later along the whole root.

Cytokinin endogenous levels increase after ESR2 induction in seedlings

The effects of ESR2 induction were similar to those caused by increased levels of cytokinins, and to ascertain the presence of an increased content of these phytohormones in the induced plants, we conducted a quantitative analysis of endogenous cytokinin levels in WT versus induced and non-induced *ESR2:ER* seedlings (Fig. 1K, Tables 1 to 5). The quantification revealed a significant

increase in total endogenous cytokinin levels (45.46 pmol/g FW ± 1.38) in *ESR2:ER* induced seedlings in comparison to *ESR2:ER* non-induced seedlings (25.84 ± 1.39) and WT seedlings (26.67 ± 1.02) (Table 1), which had a similar total cytokinin content. The cytokinin types that showed statistically significant accumulation in induced *ESR2:ER* seedlings were isopentenyl adenine (iP) and cis-zeatin (cZ) types (free bases, ribosides, and glucosides), whereas the level of some trans-zeatin (tZ) type cytokinins (free bases and ribosides) had actually decreased (Fig. 1K, Tables 2 to 4). Therefore, the induction of ESR2 leads to an increase in total cytokinin levels, particularly isopentenyl adenine and cis-zeatin species, along with a reduction of trans-zeatin free bases and ribosides.

IPT5 expression increases after ESR2 activation

Since ESR2 promotes an increase in total cytokinin endogenous levels, we investigated whether ESR2 could regulate genes involved in cytokinin biosynthesis. The first and rate-limiting step in cytokinin biosynthesis is catalyzed by ISOPENTENYL TRANSFERASES (IPTs) (Miyawaki et al., 2004, 2006). *IPT5* expression has been reported at the early stage I of lateral root development and *de novo* root development (Bustillo-Avendaño et al., 2018; Chang et al., 2015; Miyawaki et al., 2004) and during the process of callus development from roots (Atta et al., 2009). Based on this, we employed RT-qPCR to assess whether ESR2 overactivation affected *IPT5* expression. An increase in *IPT5* expression was observed while comparing WT and *ESR2:ER* seedlings treated with β-estradiol and cycloheximide (which inhibits translation) or a mock solution for 30 min at 9 Days After Germination (DAG) (Fig. S1A). Interestingly, there is a slight leakiness in ESR2:ER activity, since there was an increase in expression in the non-induced *ESR2:ER* line compared to WT plants at this early time. Nevertheless, to follow the expression at later times after induction, and visualize its spatial pattern, we analyzed the *IPT5* promoter marker line *IPT5::GUS* (Dello Ioio et al., 2008) in the *ESR2:ER* background. A clear increase in GUS signal in the vascular region of hypocotyls, cotyledons, and leaves, was observed 48 hours after ESR2 induction (Fig. 2A). It was also slightly higher in some vascular regions in non-induced *ESR2:ER IPT5::GUS* compared to the WT background (Fig. S1B), again suggesting a slight leakage of ESR2:ER activity. However, after ESR2 induction, GUS staining intensified compared to mock-treated plants and

expanded completely throughout the entire vasculature of the aerial organs (Fig. 2A). The induction of ESR2 activity also altered *IPT5* expression in roots. In mock-treated *ESR2:ER* roots, expression was equivalent to WT plants. It was detected in lateral root primordia and was maintained at their apex as the young lateral root elongated (Fig. 2D and Fig. S2A to F, Miyawaki et al., 2004), while the apex of the main root did not show *IPT5* expression. However, when ESR2 was activated, *IPT5* expression was observed in the main root apex (Fig. 2A and Fig. 2D). After 8 days, *IPT5* expression in the root tip of induced plants was lost again. This could be due to the extreme changes in its phenotype, since the root apex had increased in thickness, was disorganized, and the root apical meristem was not recognizable anymore in the induced plants, in contrast to mock-treated plants (Fig. S2G and H). Nevertheless, increased *IPT5* expression was detected in the vascular region, and six to eight days after induction, the expression had extended along the whole root as two continuous lines in the vasculature region (Fig. 2B and D), which did not happen in non-induced plants. In conclusion, ESR2 activation leads to a clear increase in *IPT5* expression.

AHP6 expression increases after ESR2 induction

ESR2 activation also promotes the ectopic expression of *HISTIDINE PHOSPHOTRANSFER PROTEIN 6* (*AHP6)*, involved in cytokinin signaling inhibition, in the gynoecium pro-vasculature (Durán-Medina et al., 2017a), and increased expression in root explants (Ikeda et al., 2006). Therefore, given its relation to the cytokinin pathway, we analyzed *AHP6* expression after ESR2 induction in seedlings through RT-qPCR and found that it increased 30 minutes after activation of ESR2 (Fig. S1A).

While analyzing the *AHP6* promoter reporter line *AHP6::GFP* (Mähönen et al., 2006) in the *ESR2:ER* background, we observed a clear increase of *AHP6* expression associated with vascular tissues of petioles and roots 48 hours after ESR2 induction, similar to *IPT5* (Fig. 2C). Interestingly, 48 hours after ESR2 induction, a broader expression domain of *AHP6* was observed in roots. *AHP6* also presented ectopic expression in epidermal cells at the root apex (Fig. 2C).

Taken together, the results indicate that ESR2 activation caused increased and ectopic expression of *IPT5* and *AHP6* in young seedlings.

The loss of *IPT5* and *AHP6* functions suppress morphological defects caused by ESR2 overactivity in a gene-dependent manner

After observing the increase in *IPT5* and *AHP6* expression due to ESR2 induction, we assessed their involvement in the phenotypes caused by ESR2 induction. For this, we analyzed how the loss of *IPT5* or *AHP6* function affected the phenotypes triggered by ESR2 activation in *ESR2:ER ipt5* or *ahp6* mutants. When ESR2 was induced at 6 DAG, seedlings presented stunted cotyledons and two true leaves that were barely visible, in contrast to mock-treated seedlings (Fig. 3A). This effect in young leaves has also been observed in constitutive *ESR2* overexpression lines (Marsch-Martinez et al., 2006). While the first two true leaves were barely visible in induced *ESR2:ER* plants, they appeared to be larger in the induced mutant backgrounds (*ESR2:ER ipt5* and *ESR2:ER ahp6)* (Fig. 3A). 17 days after germination, induced *ESR2:ER* seedlings had not formed more visible leaves in addition to the first two that remained small, in contrast to mock-treated plants where developing leaves were visible (Fig. 3A). This lack of visible developing leaves was maintained at later stages of development (Fig. S3E and F). Induced *ESR2:ER ipt5* and *ESR2:ER ahp6* seedlings had visible new leaves, resembling the phenotype of mock-treated *ESR2:ER* seedlings (Fig. 3A). This indicated that the leaf phenotypes produced by ESR2 activation require functional *IPT5* and *AHP6*.

ESR2 overactivity also affects root development. Eight days after germination in the induction medium, the main roots of *ESR2:ER* and *ESR2:ER ahp6* seedlings displayed a profusion of root hairs, while fewer root hairs were observed in *ESR2:ER ipt5* seedlings (Fig. S3A). At 13 DAG in the induction medium, the main root apex of *ESR2:ER* seedlings started to coil (Fig. S3B), and the hairy roots were still visible. Induced main roots had an average length of 1.2 cm, while mock-treated roots were 6 cm long on average (Fig. 3B). The roots of induced *ESR2:ER ahp6* seedlings still showed the profusion of root hairs (Fig. S3B) but were about 1.7 cm long on average, slightly longer in comparison to induced *ESR2:ER* roots (Fig. 3B). Interestingly, the loss of *IPT5* function in induced *ESR2:ER* seedlings allowed the development of the root comparable to non-induced seedlings lacking the profusion of root hairs (Fig. S3B) and exhibiting an average length of 6.4 cm (Fig. 3B). Therefore, the early root growth inhibition and increased root hair density promoted by ESR2 activation appear to require a functional *IPT5*, while *AHP6* seems to play a contributory role, but to a lesser extent, in young plants.

We next explored the effect of the loss of *IPT5* or *AHP6* function on ESR2-promoted callus development. Mock-treated *ESR2:ER* seedlings developed normally, while induced seedlings presented stunted shoot and root growth, and callus development (Fig. S3E). To allow evident callus development also in the mutant backgrounds, induced plants were analyzed at 40 DAG. As expected, the roots of induced *ESR2:ER* plants did not elongate further, and green calli developed along their entire root length (Fig. 3C and Fig. 3SE). *ESR2:ER ipt5* roots were less affected by ESR2 induction as they continued developing and became longer than *ESR2:ER* roots (Fig. 3C). This was already evident a few days after induction (Fig. S3B). Furthermore, *ESR2:ER ipt5* roots exhibited a marked reduction in green callus formation after induction (Fig. 3C), with the majority of plants failing to show any callus development in the entire root. In some plants, only a few small calli were formed (Fig. S3C), contrasting to the massive callus formation in induced *ESR2:ER* roots in the WT background (Fig. 3C), already observed at earlier times (Fig. S3E). Moreover, the few calli formed in *ESR2:ER ipt5* roots developed only at the base of a few lateral roots, rather than along the entire root (Fig S3D).

In the case of *ESR2:ER ahp6*, though young roots initially presented an ESR2 induction phenotype that resembled the phenotypes of induced *ESR2:ER* seedlings in a wild-type background, the altered phenotypical characteristics were lost as they developed. Induced *ESR2:ER ahp6* roots developed normally afterwards, despite the prolonged exposure to the induction medium. As occurred for induced *ESR2:ER ipt5*, their roots were longer than induced *ESR2:ER* roots (Fig. 3C). Remarkably, these *ESR2:ER ahp6* plants did not form any visible calli after ESR2 induction, not even after the extended induction period (Fig. 3C). The severe reduction or lack of callus formation in *ipt5* and *ahp6* mutants indicates that these effects caused by ESR2 induction require functional *IPT5* and *AHP6*.

When analyzing the roots of induced *ESR2:ER* seedlings in more detail, we noticed anomalies in the vascular tissues, already evident in the *IPT5* and *AHP6* reporter lines within the induced *ESR2:ER* background (Fig. 2B and C). To further investigate these anomalies, we stained the roots with basic fuchsin, which stains lignin and allows the visualization of xylem cells (Mähönen et al., 2000). In mock-treated *ESR2:ER* seedlings, two well-defined stained lines corresponding to protoxylem cells were observed (Fig. S3G), while a stained broad band was observed in the roots of induced seedlings (Fig. 3D). This suggested that ESR2 activation led to an increase in fuchsin-

stained vascular cells. Interestingly, the roots of induced *ESR2:ER ipt5* seedlings presented a reduction in xylem strands compared to induced *ESR2:ER* seedlings (Fig. 3D), with their xylem appearing to be more similar to those of mock-treated *ESR2:ER* plants. Conversely, the roots of induced *ESR2:ER ahp6* seedlings presented an even more disorganized pattern of protoxylem strands than induced *ESR2:ER* or mock-treated *ESR2:ER ahp6* roots (Fig. 3D and Fig. S3G). This indicates that *IPT5* contributes to the altered vasculature phenotype caused by ESR2 induction, while *AHP6* appears to counteract it.

In summary, functional *IPT5* and *AHP6* are required for the ESR2-induced stunted and darker leaf, late root inhibition, and callus formation phenotypes, while *IPT5* is required for the ESR2-induced altered vascular phenotype and *AHP6* counteracts it.

Cytokinin application partially restores green callus development in *ESR2:ER ipt5* roots

The previous experiments indicated that ESR2 promotes the development of green calli through the regulation of biosynthesis and negative signaling steps of the cytokinin pathway, suggesting that cytokinin plays a prominent role in ESR2-induced callus formation. Therefore, we investigated the effect of exogenous cytokinin on the inducible *ESR2:ER ipt5* and *ahp6* mutant backgrounds. We specifically evaluated whether exogenous cytokinin could compensate for the loss of *IPT5* function, by complementing the lack of cytokinin biosynthesis and restoring callus formation in the *ESR2:ER ipt5* background. We also explored the effect of exogenous cytokinin in the *ESR2:ER ahp6*, where negative signaling is compromised.

For this, seedlings were grown in media supplemented with 20 μM β-estradiol and transplanted to media with 30 μM 6-benzylaminopurine (BAP) and 20 μM β-estradiol at 6 DAG (Fig. 4A and Fig. S4A to C). Interestingly, after 34 days, all *ESR2:ER ipt5* plants presented callus formation in their hypocotyls, near the root-hypocotyl junction, and at the root apex (Fig. 4A and Fig. S4B). Callus development along the root was minimal, not at the extent observed in induced *ESR2:ER* plants, but it was evident that BAP treatments increased calli formation in these plants, in contrast with plants grown without BAP (Fig. S4A and B). In the case of *ESR2:ER ahp6* plants, most did not present visible calli, and only a few developed green root tips resembling calli (about 20%, Fig. S4B and C). Callus development occurred only at the root apex but not in other regions, like in *ESR2:ER* or BAP-treated *ESR2:ER ipt5* plants. Remarkably, instead of calli, some shoot-like

structures were observed at the base of *ESR2:ER ahp6* hypocotyls (Fig. 4A). This peculiar effect had not been observed before in any of the previous experiments and was only found in induced *ESR2:ER ahp6* plants treated with cytokinins, suggesting that in these conditions, *AHP6* suppresses shoot formation.

We next evaluated callus formation in *ESR2:ER, ESR2:ER ipt5,* and *ESR2:ER ahp6* seedlings that were directly germinated in a medium supplemented with BAP and β-estradiol. They were observed 40 days after induction. In these conditions, induced *ESR2:ER* plants became very compact, lacked visible roots, and the whole plant transformed largely into a large mass of calli (Fig. 4B). Direct germination in these conditions intensified callus formation in *ESR2:ER ipt5* plants compared to those transferred to the BAP medium after germination. They exhibited extensive callus formation (Fig. 4B), resembling induced *ESR2:ER* plants to a greater extent. Calli developed in the root, only not along the entire root as in *ESR2:ER* plants (Fig. 4B). Instead, calli developed mainly at the hypocotyl, its base, the root-hypocotyl junction, and the root apex. Again, though the formation of calli was still more pronounced in *ESR2:ER* than *ESR2:ER ipt5* plants, BAP addition to the medium promoted increased callus formation in *ESR2:ER ipt5* plants in comparison to the same plants grown in induction medium without this hormone.

ESR2:ER ahp6 seedlings presented visible roots without calli. Instead, calli developed from aerial tissues (Fig. 4B). *ESR2:ER ahp6* shoots were severely disorganized. Interestingly, besides calli, shoot-like structures, leaves, and some radialized, rod-like structures could be recognized in the aerial part of these *ESR2:ER ahp6* plants (Fig. 4B). It is worth noting that calli did not develop in any of the control plants (WT, *ahp6*, and *ipt5*) under the tested conditions. In some BAP-treated *ahp6* seedlings, a slight growth of ectopic tissue was observed in the hypocotyl. This tissue was not green, and its growth was moderate in comparison to ESR2-induced calli that had developed at the same time as green cell masses (Fig. 4B).

These experiments indicate that cytokinin biosynthesis mediated by *IPT5* has a role in the formation of callus in whole seedlings caused by ESR2 induction. Increased cytokinin levels, on the other hand, partially restored callus formation in *ESR2:ER ahp6* roots, though to a lesser extent than in *ESR2:ER ipt5*.

After observing the formation of shoots in *ESR2:ER ahp6* plants after transference to ESR2 induction medium supplemented with cytokinin, we explored the shoot regeneration capacity of

root explants by directly placing them on Shoot Inducing Medium (SIM, a cytokinin-rich medium), without pre-induction in Callus Inducing Medium (CIM). After three weeks of ESR2 induction in SIM, massive green callus development was observed in all *ESR2:ER* root explants, unlike WT root explants that became green but presented only little callus growth or *ahp6* explants that maintained their original phenotype (Fig. 4C). Interestingly, around 85% *ESR2:ER ahp6* root explants developed shoot structures instead of green calli (Fig. 4C). Like the formation of shoots at the base of the hypocotyl in induced *ESR2:ER ahp6* whole plants in the presence of cytokinins (Fig. 4A), this had not been observed in induced *ESR2:ER* plants or explants in any of our previously tested conditions. It suggested that in the absence of *AHP6* function, shoot formation can be enhanced both in whole plants and explants and the callus induction step may not be required for shoot regeneration.

Conversely, the response capacity to the cytokinin in the SIM is reduced in the absence of functional *ESR2*. In root explants of the *drnl-2* loss of function mutant, where *ESR2* function is lost, no severe changes were observed after transference to SIM, in contrast to WT explants, which became green and showed moderate cell proliferation (Fig. 4D and Fig. S5A and B). To investigate whether increasing cytokinin concentration could increase the effect in *drnl-2*, BAP was directly added to the explants. After 10 days of the BAP treatment, we observed a slight increase in green coloration in *drnl-2* explants, suggesting a partial restoration of the greening effect seen in WT explants (Fig. S5C).

ESR2 can bind to *IPT5* and *AHP6* regulatory regions and activate their expression

After confirming that both *IPT5* and *AHP6* were upregulated and contributed to the phenotypic alterations caused by ESR2 overexpression, we explored the nature of the regulation of *IPT5* and *AHP6* by ESR2. The RT-qPCR experiments in seedlings treated with cycloheximide suggested a possible direct regulation; hence, to further investigate this possibility, we employed Yeast-1-Hybrid and NanoLuc transactivation assays. Many AP2/ERF-type transcription factors recognize a conserved binding site, the GCC box (Fujimoto et al., 2000; Hao et al., 1998; Ohme-Takagi & Shinshi, 1995). Previous works have shown that ESR2 binds to and regulates targets through a

GCC box (Eklund et al., 2011; Zhang et al., 2018). Using the Plant Promoter Analysis Navigator (PlantPAN; http://PlantPAN.itps.ncku.edu.tw/ (Chow et al., 2019)), we identified one GCC box at -289 bases from the *IPT5* ATG (pink diamonds in Fig. 5A). In addition, three other sequences related to the GCC box were also identified in *IPT5*, two of them within the *IPT5* ORF, 10 and 18 bases near the translation stop codon and another in the 3' UTR (purple diamonds, Fig. 5A). We considered these regions as potential ESR2 binding sites and evaluated them using Y1H assays. We tested two fragments comprising the complete region upstream from the ATG, A 1945 bp (fragment I) and a 70 bp long fragment that contained the GCC box (fragment II). In addition, a fragment of 532 bp that included the three GCC boxes located at the end of the *IPT5* ORF and its 3' UTR (fragment III) was also tested. The results of the Y1H assays revealed an interaction between ESR2 and the 3 fragments (Fig. 5B).

In the case of the *AHP6* promoter, we identified two boxes at -258 and -293 bases from the start codon (pink diamonds) (Fig. 5A). Through the Y1H assay, we aimed to test five *pAHP6* promoter fragments, including fragments I to III (450 bases each), fragment IV (527 bp), and V (a small fragment of 100 bp) containing the region of GCC boxes (Fig. 5A). However, fragments I, IV and V presented auto-activation (the activation of reporter genes without the participation of the transcription factor) and could not be tested (Fig. S6). Promoter fragments II and III did not show autoactivation and the Y1H assays revealed ESR2 interaction with them (Fig. 5B).

We then validated the regulation of *IPT5* and *AHP6* by ESR2 *in planta* using a transient luciferase assay. We tested promoter fragments comprising 1945 bp upstream of the ATG of *IPT5*, and 1900 bp upstream of the ATG of *AHP6*. Both promoter fragments were fused to the bioluminescence reporter NanoLuc (NL). These constructs were transiently expressed in tobacco leaves together with a *35S::ESR2* construct. In the absence of the *35S::ESR2* construct, we detected very little NanoLuc activity (Fig. 5C). However, when *35S::ESR2* was co-infiltrated with *pIPT5::NL* or *pAHP6::NL*, a clear increase in bioluminescence was detected (Fig. 5C). The results of both the Y1H and NanoLuc experiments suggest direct binding and activation of *pIPT5* and *pAHP6* by ESR2.

Subsequently, to investigate whether the regulation of ESR2 towards *IPT5* and *AHP6* could occur in the natural context of *ESR2* expression, we compared their natural expression patterns during

seedling development. We explored *IPT5* expression using the *IPT5::GUS* promoter reporter line and compared it with the *ESR2* promoter marker line *BOL::GUS* (Marsch-Martinez et al., 2006). Visualization of stained *IPT5::GUS* whole seedlings revealed overlapping in some tissues where *ESR2* is also expressed (Fig. 5D and Fig. S7A and B). High overlapping between *ESR2* and *IPT5* expression could be mainly observed in young leaf tissues, particularly leaf vasculature at very early stages of development and stipules (Fig. 5D and Fig. S7A and B). In more developed tissues, differences in expression patterns were evident since *IPT5* was expressed in the vasculature of cotyledons and leaves at later stages of development, while the expression of *ESR2* remained confined to discrete points in the apex of young leaves and cotyledons (Fig. S7A and B).We also analyzed *AHP6* expression using the *AHP6::GFP* reporter line and compared it to a genomic reporter line, *ESR2::ESR2:GFP*. As previously reported, *ESR2* expression was observed in the meristem peripheral zone, at the region where a new leaf primordium will emerge, and in leaf primordia (Fig. 5D and Figure S7C and D, Ikeda, et al., 2006a; Marsch-Martinez et al., 2006b; Nag et al., 2007). Moreover, *ESR2* expression was also observed in tissues such as the tip of leaf primordia, the developing main vasculature of the youngest leaves, and the stipules (Fig. 5D and Fig. S7A). *AHP6* expression coincided in some regions of leaf primordia, stipules, and the developing vasculature of young leaves (Fig. 5D and Fig. S7D). In summary, these results suggest that the regulatory effect of ESR2 upon *IPT5* and *AHP6* could be direct and that these genes might be natural targets in specific tissues of the plant, such as the stipules and young vasculature for *IPT5*, and these tissues plus the tip of leaf primordia for *AHP6*.

DISCUSSION

Our study aimed to determine whether the transcription factor ESR2 could modulate the cytokinin pathway positively to promote callus development. Callus formation plays a crucial role in indirect regeneration (reviewed by Ikeuchi et al., 2013, 2019) and can be triggered by specific ratios of the phytohormones cytokinin and auxin. Subsequently, shoot regeneration occurs under high cytokinin to low auxin ratios (reviewed in Ikeuchi et al., 2019; Skoog & Miller, 1957). Different studies have focused into understanding these two processes, though many aspects are still unknown (reviewed in Shin et al., 2020).

Loss of *ESR2* function reduces the capacity of Arabidopsis hypocotyl and root explants to regenerate shoots *in vitro* (Matsuo et al., 2011). Moreover, ESR2 has a remarkable ability to induce green callus formation and shoot regeneration even without the addition of exogenous hormones (Ikeda et al., 2006a; Marsch-Martinez et al., 2006) and the effects of ESR2 induction are comparable to those observed with cytokinin treatments or increased cytokinin content in plants. Other lines of evidence further suggest a potential positive role of ESR2 in cytokinin-related processes. ESR2, together with REVOLUTA (REV), positively regulates *SHOOT MERISTEMLESS (STM)* (Zhang et al., 2018), and STM promotes cytokinin biosynthesis by activating the expression of *IPT7* (Jasinski et al., 2005; Yanai et al., 2005). Moreover, alterations in the effects of cytokinin treatments in young gynoecia of *drnl-2* (an *ESR2* loss-of-function allele (Nag et al., 2007)) mutants indicated a positive role in the early developmental stages of this important reproductive organ (Durán-Medina, et al., 2017a). Furthermore, global expression analyses in *lfs* (loss of function of the only *ESR2* homolog in tomato) also supported a potential positive effect of *ESR2* on the cytokinin pathway (Capua & Eshed, 2017).

In line with these observations, when we measured different cytokinin forms in ESR2-induced plants, a clear increase in total cytokinins was observed, especially iP and cZ types. In particular, iP types have been associated with the ability of cytokinins to promote root primordia disorganization and shoot identity (Pernisova et al., 2018); these effects are also observed in ESR2 overexpressors. Isopentenyltransferases (IPTs) catalyze a critical step in cytokinin biosynthesis, and *ipt* mutants have reduced levels of iP and tZ types (Miyawaki et al., 2006), while *IPT* activation lines or overexpressors predominantly exhibit an increase in iP types (Kakimoto, 2001; Sun et al., 2003; Zubko et al., 2002). Increased *IPT* expression enhances shoot regeneration and leads to phenotypes such as green callus formation in cytokinin-free conditions, shorter roots, and dark green cotyledons (Kakimoto, 2001; Sun et al., 2003; Zubko et al., 2002). These phenotypic similarities with ESR2/BOL overexpression lines (Ikeda et al., 2006; Marsch-Martinez et al., 2006) and the higher iP-type cytokinin content, pointed to *IPTs* as potential downstream genes responsible for the increased cytokinin content and related phenotypes associated with ESR2. In tissue culture, callus formation has been linked to a lateral root development program (Atta et al., 2009; Sugimoto et al., 2010). *IPT5*, among the potential candidate *IPTs*, exhibits increased expression during the early stages of both lateral root and callus formation (Atta et al., 2009), and showed upregulation in roots and shoots. This response might have been overlooked in

previous studies because of a slight ESR2 activity leakage in the inducible line, and a very modest increase in expression at short times after induction. Nevertheless, *IPT5* expression gradually intensified at longer times after ESR2 induction, showing a very sharp increase and coinciding with the formation of calli triggered by ESR2 induction, in contrast with mock-treated plants where only a very modest increase in expression and normal root development were observed. Intriguingly, while ESR2 induction caused increased *IPT5* expression and cytokinin content, *AHP6*, a negative regulator of cytokinin signaling (Mähönen et al., 2000), has also been found to be activated by ESR2 in other tissues. ESR2 activates *AHP6* in root explants (Ikeda et al., 2006); in young gynoecia and inflorescences (Durán-Medina et al., 2017a); and has been found as an ESR2 target in lateral organ founder cells (Frerichs et al., 2019). The results obtained in the Y1H and transient expression experiments further suggested that ESR2 binds and activates the promoters of *IPT5* and *AHP6* directly. Notably, *AHP6* has been recently found to be a direct target in inflorescence meristems (Dai et al., 2023).

Therefore, interestingly, ESR2 induction can activate both cytokinin biosynthesis (*IPT5)* and signaling inhibition (*AHP6*), and some ESR2-induction phenotypes, such as initial root growth inhibition, were differently affected by the loss of each gene. However, despite their seemingly contradictory effects in the cytokinin pathway, both functional *IPT5* and *AHP6* are essential to obtain other ESR2-induced phenotypes, such as stunted leaf formation. Remarkably, they are both required for the massive green calli formation in roots, one of the most conspicuous phenotypes caused by ESR2 activation. This suggests that ESR2-mediated callus induction requires a delicate balance between an increase in cytokinin content and a reduction in cytokinin signaling in the regions where *AHP6* expression is upregulated.

Cytokinins are known to move from cell to cell (reviewed by Durán-Medina et al., 2017b; Liu et al., 2019). Free CK bases, the biologically active forms, have been proposed to diffuse through cell membranes (Nedvěd et al., 2021). Building on this knowledge, we propose a hypothetical scenario to explain the dual requirement for cytokinin biosynthesis and signaling inhibition during ESR2-induced callus development, in which ESR2-responsive regions are established where cytokinins are produced (Fig. 6). These regions would serve as local sources for cytokinin synthesis, which then would be mobilized through transport or diffusion to neighboring cells. Simultaneously, cytokinin signaling is selectively reduced within the ESR2-responsive region.

However, this reduction does not extend to neighboring cells, which respond to the cytokinin produced in the adjacent source regions, creating differential CK response fields. ESR2 would then modulate the delicate balance between cytokinin production and localized signaling inhibition, which would lead to callus formation in this system.

We hypothesize that this formation of cytokinin content and signalling/response "fields" could occur in the region of the vascular tissues, as we have observed increased expression of both genes at the same time in this region, upon induced overexpression of ESR2. From the vascular and vascular-related tissues, we speculate that it may take place at the xylem pericycle, a tissue shown to originate callus formation from the root and other tissues (Atta et al., 2009, Sugimoto et al., 2010, Che et al., 2007, Laplaze et al., 2005), or the cambium.

More detailed studies should provide the necessary evidence to support this hypothetical model, and the precise cellular context in which it takes place, if confirmed. Moreover, we cannot exclude the possibility that it could also be taking place in the tissue context in which *ESR2*, *IPT5* and *AHP6* are naturally expressed in natural or *in vitro* regeneration conditions, and future work can also shed light in this matter.

Such positive-negative cytokinin regulation modules exist in other plant tissues. Positive regulation of both cytokinin biosynthesis and negative signaling or degradation is required for proper vascular development. The TARGET OF MONOPTEROS 5/LONELY HIGHWAY (TMO5/LHW) dimer activates cytokinin biosynthesis through *LONELY GUY 3* and *4 (LOG3* and *4*) and reduces cytokinin signaling through the activation of *AHP6* in xylem precursor cells (Ohashi-Ito et al., 2014, De Rybel et al, 2016). Moreover, the TMO5/LHW dimer also activates cytokinin degradation indirectly via *CKX3* expression in adjacent cells (Yang et al., 2021). Curiously, *ESR2* has also been reported to be a target of MONOPTEROS (MP) (Dai et al., 2023), and a similar scenario could occur in the case of ESR2-induced calli (Fig. 6), which warrants investigating whether this is the case, in these and other calli, or other tissues.

Differences in the recovery of callus formation were observed in *ESR2:ER ahp6* and *ESR2:ER ipt5* mutants when supplemented with cytokinins, since this ability was recovered to a greater extent in *ESR2:ER ipt5* than in *ESR2:ER ahp6* plants. This was expected given the contrasting

functions of *IPT5* and *AHP6*. Interestingly, in the induced *ESR2:ER ahp6* supplemented with cytokinins, radialized aerial organs were formed, reminiscent of the ones observed in *drn-D*, the activation tagging line of one of the homologs to ESR2, ESR1/DRN, gain-of-function mutants (Kirch et al., 2003). Moreover, shoot formation in the hypocotyl-root junction was obtained in these lines, which was never observed before in *ESR2:ER* whole seedlings in the wild-type background, where only calli develop after induction. Induced *ESR2:ER ahp6* grown directly in SIM medium, without any previous step in CIM, also developed shoots, while *ESR2:ER* explants in the same conditions produced a profusion of green calli. Therefore, *AHP6* could be contributing to the inhibition of proper shoot regeneration from green calli in these seedlings.

Cytokinin treatments alone were not enough to trigger equivalent ESR2-induced callus formation in mock-treated *ESR2:ER* (or WT, *ipt5* or *ahp6* plants) under any treatment, indicating that the increase in cytokinin availability in these lines is not enough to induce calli. Most likely, ESR2 regulates other processes in combination with cytokinin biosynthesis and signaling inhibition, which are also required for callus development. One of these processes could be related to auxin (Chandler et al., 2011; Chandler & Werr, 2014; Skoog & Miller, 1957). ESR2 activates *SHORT INTERNODES/STYLISH* (*SHI/STY*) (Eklund et al., 2011), which in turn activates auxin biosynthesis (Sohlberg et al., 2006). Nevertheless, future studies should identify the other genes (including other auxin or cytokinin-related genes) and processes that are involved in ESR2-induced callus formation.

Curiously, while the induced activation of ESR2, whose expression is driven by a 35S promoter, was expected to upregulate *IPT5* and *AHP6* indistinctly in many plant tissues, the upregulation of both genes was mostly restricted to the vascular region (in the analyzed roots and shoots). This might indicate that other factors, including epigenetic marks or interacting transcription factors, among others, restrict the action of ESR2 on these genes and confine it to the vascular tissues. Moreover, the induced plants also presented an enlarged vascular region (Fig. 3D). Cytokinins promote procambial cell proliferation and secondary growth (Matsumoto-Kitano et al., 2008; Ye et al., 2021). The increased number of vascular cells observed after ESR2 induction was reduced in the *ipt5* mutant, suggesting that it could be due to an increase in cytokinin biosynthesis. Conversely, the lack of *AHP6* function exacerbated the phenotype, observed as a larger region of lignified cells, possibly due to an increased sensitivity to the high cytokinin content.

Natural context and relevance of regulation

We studied the regulation of the *IPT5* and *AHP6* cytokinin genes by ESR2 in the context of its ability to induce callus formation and other cytokinin-related phenotypes when overexpressed, and it is possible that this regulation could occur in a natural context. Co-expression can provide insights into where this regulation could occur naturally.

Expression of both *ESR2* and *AHP6* has been reported in founder cells of floral organs (Besnard et al., 2014; Chandler et al., 2011), where the regulation could occur naturally, and, accordingly, ESR2 has been confirmed to activate *AHP6* in the inflorescence shoot meristem (Dai et al., 2023).

Interestingly, we observed co-expression of *ESR2*, *AHP6*, and *IPT5* in the often-overlooked stipuli within the developing primordia of the vegetative shoot apical meristem. Their function remains largely unknown, but they have been implicated as sites of diffusible signal production (Oppenheimer et al., 1991). It would be interesting to further investigate whether the expression of these three genes indicates that stipuli could be an insensitive reservoir of cytokinins, capable of diffusing to the developing organs or even the SAM.

Another region reflecting the coincidence of the three genes was the vasculature of developing leaves. Coupled with the sharp increase in *IPT5* and *AHP6* expression upon ESR2 induction in the vascular region, this observation hints at ESR2´s potential role in naturally activating these genes in this region. Interestingly, ESR2 was found, and recently confirmed to directly activate *CKX7* (Dai et al., 2023; Ikeda et al., 2006), which is also expressed in the vasculature (Köllmer et al., 2014). We could speculate that ESR2 may also have a role in promoting the formation of differential cytokinin content or sensibility fields during vascular development, by inducing cytokinin biosynthesis and promoting insensibility or degradation in the cells where it is expressed. Again, further research is required to provide evidence to support this suggestion. Interestingly, a previously unidentified role for ESR2/DRNL in vascular development has been recently uncovered, supporting this hypothesis (Glowa et al., 2021), and the increased number of vascular cells after ESR2 induction also suggests ESR2's role in this process. Nevertheless, it is also possible that the regulation of *IPT5*, *AHP6*, and *CKX7* by ESR2 occurs at different stages or tissues

(for example, during flower or floral organ development), and this should be explored in further detail in other investigations.

In summary, ESR2 influences both cytokinin levels and local cytokinin signaling inhibition that leads to callus formation and other phenotypes. More research will shed light on the cellular implications of this regulation and whether this also occurs other tissues.

MATERIALS AND METHODS

Plant materials and growth conditions

The lines used in this study were: Columbia (Col-0) wild-type plants; *ipt5-2* (Miyawaki et al., 2006) and *ahp6-1* mutants (Mähönen et al., 2006, genotyped as in Muller et al., 2017); *pBOL::BOL:GFP* (this work, renamed as *ESR2::ESR2:GFP*), *BOL::GUS* (Marsch-Martínez et al., 2006) , *IPT5::GUS* (Dello Ioio et al., 2008), and *AHP6*::*GFP* (Mähönen et al., 2006); and the inducible ESR2 line *35S::ESR2-ER* (Eklund et al., 2011; Ikeda et al., 2006), mentioned in this work as *ESR2:ER*. More information in the Supplementary Material and methods section.

ESR2::ESR2:GFP reporter construct and line

A 6 kb fragment containing regulatory sequences upstream the ATG of *DRNL/ESR2/BOL* and the coding region until just before the stop codon was amplified from wild type Col-0 DNA, with primers IC36 and IC37 (Table S1), using Phusion polymerase (New England Biolabs) and cloned in the pENTR/D-TOPO vector, using the cloning kit (Invitrogen). The fragment was confirmed by sequencing, and the promoter fragment was recombined using Gateway LR Clonase Enzyme mix (Invitrogen) into the pMDC204 vector (Curtis & Grossniklaus, 2003), resulting in construct *ESR2::ESR2:GFP*. The resulting binary vector was transformed to *A. tumefaciens* pGV2206 and, using a modified floral dip method, introduced in *drnl-2* (Nag et al., 2007) plants. Transformants were selected in hygromycin-containing medium.

Histology and microscopy

ESR2:ER induction was either performed in 6 DAG seedlings germinated in 0.5x MS medium and transferred to medium supplemented with 10 μM β-estradiol, or germinated directly in the latter medium, and compared to those transplanted to or germinated in mock MS medium supplemented only with DMSO (the solvent used to dissolve β-estradiol). To determine the regulation of *AHP6* and *IPT5* expression in response to ESR2 induction in specific tissues, crosses between *ESR2:ER* and *AHP6::GFP* or *IPT5::GUS* expression marker lines were obtained. Homozygous *ESR2:ER AHP6::GFP* and *ESR2:ER IPT5::GUS* seedlings were transplanted to MS medium with 10 μM β-estradiol (Sigma–Aldrich). Treated seedlings were removed from the plates and processed for expression visualization 48 hours after ESR2 induction. More information in the Supplementary methods section.

Quantification of endogenous cytokinins

Quantification of CK metabolites was performed as previously described in (Svačinová et al., 2012). Seeds of Col-0 and *ESR2:ER* were stratified in MS medium (Murashige & Skoog, 1962) and germinated in petri dishes in a growth chamber (22°C and 16 hours-light). Five days after germination, seedlings were transferred to MS with 10 μM β-estradiol (treatment medium) and MS without β-estradiol ("Mock" medium) and grown in the same conditions as before. Two weeks after the transference, around 20 mg of the treated and mock seedlings were harvested. They then were frozen with liquid nitrogen and stored at -80°C; Four independent biological replicates were harvested for each genotype and treatment. Samples (20-30 mgFW) were extracted in 1.0 mL modified Bieleski buffer (60% MeOH, 10% HCOOH and 30% H_2O) together with a cocktail of stable isotope-labeled internal standards (0.25 pmol CK bases, ribosides, N-glucosides, and 0.5 pmol CK O-glucosides and nucleotides were added per sample). The extracts were purified using multi-StageTips (containing C18/SDB-RPSS/Cation-SR layers), the eluates were then evaporated to dryness in a vacuum and stored at -20°C. Cytokinin levels were determined using ultra-high performance liquid chromatography-electrospray tandem mass spectrometry (UHPLC-MS/MS) using stable isotope-labeled internal standards as a reference. Statistical analysis was performed using the Student's t-test (*$p < 0.05$, **$p < 0.01$, ***$p < 0.001$).

Gene expression analysis by RT-qPCR

For RT-qPCR analysis, nine days old (DAG) Columbia and *ESR2:ER* seedlings were sprayed with different solutions: (a) 10 µM β-estradiol and 30 µM cycloheximide (CHX), (b) 30 µM cycloheximide, and (c) DMSO (solvent) in distilled water. Solution (a) was the inductor solution, β-estradiol promotes nuclear transport of the chimeric ESR2:ER transcription factor, while solution (b) and (c) were used as mock. Cycloheximide was used to prevent new protein synthesis. Aerial tissue was collected 30 minutes after treatment application. Table S1 includes the sequences of the primers used. More information in the Supplementary Material and methods section.

Calli development evaluation and cytokinin treatments

To analyze the relevance of *AHP6* and *IPT5* in ESR2-promoted callus development, crosses were made between *ESR2:ER* and the *ahp6-1* and *ipt5-2* mutants. The *ahp6-1* allele was genotyped according to (Müller et al., 2017) and *ipt5-2* was genotyped by PCR using gene and T-DNA specific primers. For the evaluation of callus development, Col WT, *ESR2:ER*, single mutant alleles, *ESR2:ER ahp6* and *ESR2:ER ipt5* seedlings were grown in MS 0.5x medium with 20 µM β-estradiol and callus development was evaluated after 40 days. To test the effect of cytokinin in the recovery of callus formation, the same seedlings were grown in MS 0.5x medium with 20 µM β-estradiol and at 6 DAG were transplanted to medium with 20 µM of β-estradiol and 30 µM of 6-benzylaminopurine (BAP, Duchefa Biochemie) or medium with 20 µM of β-estradiol and the mock solution NaOH (0.2 N, which was the solvent used for BAP), or were germinated directly in these media. More information in the Supplementary Material and methods section.

Regeneration assays

Root explants from 7-day old seedlings were cut into 5 to 6 mm segments and then transferred to Shoot Inducing Medium (SIM) to induce shoot formation. No Callus Inducing Medium (CIM) was used before transfer. The composition of the SIM medium was MS salts, 1% sucrose, Gamborg's B5 vitamins, 0.3 mg/l indole butyric acid (IBA), 0.5 mg/l trans-zeatin, and 1.5% agar. To induce the activity of ESR2, the SIM was supplemented with 20µM β-estradiol. To evaluate the effect of

a higher cytokinin concentration than the one already present in the SIM, in the *drnl-2* line, 20µL of BAP (3 mg/ml) was added directly to the root explants 20 days after transplanting them to SIM.

Promoter analyses

In silico analyses of the *AHP6* and *IPT5* regulatory sequences were made with the Plant Promoter Analysis Navigator (PlantPAN**;** http://plantpan.itps.ncku.edu.tw/plantpan3/, (Chow et al., 2019)**)** to identify putative GCC box-like regulatory element sequences.

Y1H assays

The binding of ESR2 to the promoter regions of putative target genes was tested using a Yeast one-hybrid system (Y1H), based on the Matchmaker Gold Yeast One-Hybrid protocol (https://www.takarabio.com). Promoter regions of *IPT5* and *AHP6* (Fig. 5A) were amplified using primers indicated in Table S1. Examples of autoactivation tests with different Aba concentrations, and controls are shown in Figure S6A to C. See Supplementary Material and methods.

NanoLuc activity assays

Promoters of *IPT5* and *AHP6* were recombined into the binary vector pGWB601-NL3F10H (Urquiza-García & Millar, 2019) using LR clonase mix (Invitrogen), resulting in the *pAHP6::*NL and *pIPT5::*NL reporter constructs, which were transformed into *Agrobacterium tumefaciens* GV3101. Transient assays were performed as described in (Becerra-García et al., 2023). A non-target promoter (*At3g61880*, Sotelo-Silveira et al., 2013) and the empty vector were also included in the assay as negative controls (Fig S6D). See Supplementary Material and methods.

Accession Numbers

Sequence data from this article can be found in the data libraries under the following accession numbers:

IPT5 – NCBI Gene ID: 832023, AT5G19040 (TAIR and Araport), and Q94ID2 · IPT5_ARATH (UniProt);
AHP6 – NCIB Gene ID: 844350, AT1G80100 (TAIR and Araport), and Q104N3 · Q104N3_ARATH (Uniprot);
CKX7 – NCBI Gene ID: 832248, AT5G21482 (TAIR and Araport), and Q9FUJ1 · CKX7_ARATH (UniProt).

Author contributions

Conceptualization, YDM, NMM; Methodology, YDM, HHU, JECV, LC, ON, SdF, NMM; Validation, YDM, DDR, MDM, AGF, BERC, JIRO, JECV, HGL, ON; Formal analysis, DDR, MDM, JECV, HGL, NMM; Investigation, YDM, DDR, HHU, MDM, JECV, ON; Writing – original draft, YDM, NMM; Writing – review and editing, YDM, NMM; Visualization, YDM, DDR, HGL, BERC, NMM; Supervision, LC, ON, SdF, NMM; Project administration, NMM; Funding acquisition, NMM, LC, SdF, ON.

Funding

The NMM Laboratory acknowledges the funding obtained through the CONAHCyT (earlier CONACYT, now SECIHTI Mexico) CF-2023-G-219 project, postdoc fellowships to YDM and DDR, and Ph.D. fellowships to HGL (1008711) and BERC (707345). The SdF laboratory was financed by the CONAHCYT grants FC-2015-2/1061 and CB-2017-2018-A1-S-10126. SdF is grateful for the Fellowship of the Marcos Moshinsky Foundation (2018). LC thanks the European Union project H2020-MSCA-RISE-2020 EVOfruland (101007738) for funding.

Acknowledgements

The authors thank Carlos A., Vazquez, Juan Carlos Ochoa Sánchez, Miriam Salvador Daniel, Elizabeth Mendoza Bravo, Francesco Florio, Joanna Serwatowska, Rosa Esmeralda Becerra, Juan Ramos and Vincent Cerbantez Bueno for technical help and material contribution. We are also grateful to Thomas Jack (*drnl-1* seed), Eva Sundberg (*ESR2:ER* seed), and Raffaelle Dello Ioio (for *IPT5::GUS* seed). NMM, SdF colaborate in the European Union project H2020-MSCA-RISE-2020 EVOfruland (101007738).

Declaration of interests

The authors declare no conflicts of interest.

Tables

Table 1. Profile of total cytokinins and cytokinin forms in Col-0, and ESR2-ER (mock and induced) seedlings.

Genotype	Total Cytokinins			CK Bases			CK Ribosides			CK Nucleotides			CK O-glucosides			CK N-glucosides		
Col-0	26.667	±1.018		0.236	±0.021		0.652	±0.078		5.773	±0.789		2.575	±0.145		17.431	±0.400	
ESR2 MOCK	25.845	±1.386		0.199	±0.023	*	0.588	±0.047		5.800	±0.589		2.461	±0.211		16.798	±1.233	
ESR2 Induced	45.461	±1.379	***	0.273	±0.032		1.573	±0.282	***	13.180	±1.017	***	4.495	±0.386	***	25.940	±1.648	***

The data are in picomoles per gram of fresh weight; means ± SD (n = 4). Statistical analysis was performed using Student's t test. Asterisks indicate statistically significant differences (Student's T-test * $p < 0.05$, ** $p < 0.01$, and *** $p < 0.001$).

Table 2. Profile of isopentenyladenine forms in Col-0 and ESR2-ER (mock and induced) seedlings.

Genotype	Total iP-types			iP			iPR			iPRMP			iP7G			iP9G		
Col-0	8.244	±0.248		0.071	±0.016		0.283	±0.030		2.179	±0.212		4.919	±0.294		0.792	±0.028	
ESR2 MOCK	8.570	±0.878		0.044	±0.005	*	0.291	±0.041		2.516	±0.585		4.935	±0.371		0.784	±0.038	
ESR2 Induced	18.345	±0.670	***	0.118	±0.024	*	1.087	±0.182	***	6.198	±0.525	***	9.408	±0.569	***	1.534	±0.089	***

The data are in picomoles per gram of fresh weight; means ± SD (n = 4). Total isopentenyladenine cytokinins (Total IP-types), isopentenyladenine (iP), isopentenyladenine riboside (IPR), isopentenyladenine riboside-5'-monophosphate (IPRMP), isopentenyladenine 7-glucoside (IP7G), isopentenyladenine 9-glucoside (IP9G). Asterisks indicate statistically significant differences (Student's T-test * $p < 0.05$, ** $p < 0.01$, and *** $p < 0.001$).

Table 3. Profile of trans-Zeatin forms in Col-0 and ESR2-ER (mock and induced) seedlings.

Genotype	Total tZ-types			tZ			tZR			tZRMP			tZOG			tZROG			tZ7G			tZ9G		
Col-0	9.732	±0.556		0.066	±0.020		0.207	±0.043		0.894	±0.199		1.385	±0.093		0.110	±0.018		3.902	±0.305		3.168	±0.268	
ESR2 MOCK	9.043	±0.632		0.057	±0.008		0.158	±0.015		0.752	±0.159		1.232	±0.160		0.100	±0.005		3.581	±0.334		3.163	±0.349	
ESR2 Induced	8.026	±1.230	*	0.022	±0.006	**	0.044	±0.010	***	<LOD			0.690	±0.082	***	0.171	±0.015	***	4.159	±0.486		2.939	±0.665	

The data are in picomoles per gram of fresh weight; means ± SD (n = 4). Total trans-Zeatin (total tZ types), trans-Zeatin (tZ), trans-Zeatin riboside (tZR), trans-Zeatin riboside-5´-monophosphate (tZRMP), trans-Zeatin-O-glucoside (tZOG), trans-Zeatin riboside-O-glucoside (tZROG), trans-Zeatin-7-glucoside (tZ7G), and trans-Zeatin-9-glucoside (tZ9G). Asterisks indicate statistically significant differences (Student's T-test * $p < 0.05$, ** $p < 0.01$, and *** $p < 0.001$).

Table 4. Profile of cis-Zeatin forms in Col-0 and ESR2-ER (mock and induced) seedlings.

Genotype	Total cZ-types			cZ			cZR			cZRMP			cZOG			cZROG			cZ7G			cZ9G
Col-0	7.66 3	±0.398		0.099	±0.011		0.162	±0.015		2.699	±0.420		0.247	±0.016		0.833	±0.047		3.623	±0.114		<LOD
ESR2 MOCK	7.241	±0.587		0.098	±0.019		0.139	±0.015		2.531	±0.207		0.250	±0.027		0.879	±0.049		3.344	±0.368		<LOD
ESR2 Induced	18.473	±0.815	***	0.133	±0.014	**	0.441	±0.101	***	6.982	±0.619	***	0.440	±0.016	***	3.194	±0.457	***	7.284	±0.201	***	<LOD

The data are in picomoles per gram of fresh weight; means ± SD (n = 4). Total cis-Zeatin (total cZ types), cis-Zeatin (cZ), cis-Zeatin riboside (cZR), cis-Zeatin riboside-5'-monophosphate (cZRMP), cis-Zeatin-O-glucoside (cZOG), cis-Zeatin riboside-O-glucoside (cZROG), cis-Zeatin-7-glucoside (cZ7G), and cis-Zeatin-9-glucoside (cZ9G). Asterisks indicate statistically significant differences (Student's T-test * $p < 0.05$, ** $p < 0.01$, and *** $p < 0.001$).

Table 5. Profile of dihydrozeatin species in Col-0 and ESR2-ER (mock and induced) seedlings.

Genotype	Total DHZ-types			DHZ	DHZR	DHZRMP	DHZOG	DHZROG	DHZ7G			DHZ9G		
Col-0	1.027	±0.161		<LOD	<LOD	<LOD	<LOD	<LOD	0.962	±0.152		0.065	±0.010	
ESR2 MOCK	0.992	±0.084		<LOD	<LOD	<LOD	<LOD	<LOD	0.921	±0.085		0.071	±0.008	
ESR2 Induced	0.616	±0.142	**	<LOD	<LOD	<LOD	<LOD	<LOD	0.572	±0.136	**	0.044	±0.009	*

The data are in picomoles per gram of fresh weight; means ± SD (n = 4). Total dihydrozeatin (DHZ); dihydrozeatin riboside (DHZR), dihydrozeatin riboside-5'-monophosphate (DHZRMP), dihydrozeatin O-glucosides (DHZOG); dihydrozeatin riboside-O-glucoside (DHZROG), dihydrozeatin 7-glucoside (DHZ7G), dihydrozeatin 9-glucoside (DHZ9G). Asterisks indicate statistically significant differences (Student's T-test * $p < 0.05$, ** $p < 0.01$, and *** $p < 0.001$).

Figure legends

Figure 1. **Effects of ESR2 overactivity in Arabidopsis seedling development. A)** Aerial tissue of mock and **B)** induced seedlings 15 days after ESR2 induction with β-estradiol (β-est). **C)** Closeup of the younger leaves in mock and **D)** induced seedlings 15 days after ESR2 induction. **E)** Comparison between roots of induced and mock treated seedlings. **F)** Calli developing from the tissue near or at the base of young lateral roots 21 days after ESR2 induction. **G)** Closeup of the main root apex of induced seedlings. **H)** Disorganization of lateral root emergence in induced seedlings. **I)** Average number of lateral roots, n = 30. Mann-Whitney test, $**p \leq 0.001$. Error bars represent SE. **J)** Average of primary root length, n = 30. Student's t-test, $*** p \leq 0.0001$. **K)** Cytokinin levels in wild-type (WT) and ESR2 induced and not induced seedlings. n = 4Student's t-test, *, **, and ***, $p \leq 0.01$, $p \leq 0.001$, and $p \leq 0.001$, respectively. Error bars represent SD. (iP = isopentenyladenine, tZ = trans-Zeatin, cZ = cis-Zeatin, DHZ = dihydrozeatin, iP7G = isopentenyladenine-7-glucoside, tZ7G = trans-Zeatin-7-Glucoside, cZ7G = cis-Zeatin-7-Glucoside, DHZ7G = dihydrozeatin-7-Glucoside, iPR = isopentenyladenine riboside, tZR = trans-Zeatin riboside, cZR = cis-Zeatin riboside, DHZR = dihydrozeatin riboside). Scale bars (A-D, G, H) 500 µm, (E) 1 cm and (F) 1 mm.

Figure 2. *IPT5* and *AHP6* regulation by ESR2 in aerial and root vascular tissues. A) *IPT5* expression in aerial tissue and the root tip of mock treated and induced *ESR2::ER* plants, 48 hours after treatment. **B)** *IPT5* expression in the vasculature of the *ESR2::ER* main root after 8 days of ESR2 induction. **C)** *AHP6* expression in aerial tissue and the root tip 48 hours after ESR2 induction compared to mock-treated seedlings. **D)** Sequential changes in *IPT5* expression in the main root from 2 to 8 days after ESR2 induction (dai). *IPT5* is not expressed at the root apex in non-induced seedlings, but it can be detected after ESR2 induction for a few days, and then it disappears again, as the root apex loses its organization (Fig. S1G and H). *IPT5* expression increases and expands along the vascular region of the root with time. Arrows indicate first signs of *IPT5* ectopic expression in the root after ESR2 induction. Scale bars A) 0.5 mm in aerial tissue, 0.05 mm in roots; B) 0.02 mm; C) 0.02 mm; D) 0.2 mm (top pictures) and 0.05 mm in (bottom pictures). β-est, β-estradiol.

Figure 3. Effects of *IPT5* and *AHP6* loss of function in the ESR2 activation phenotype. A) Aerial tissue development in wild type, *ahp6* and *ipt5* mutant backgrounds at 6 and 17 days after germination (DAG). Mock-treated seedlings compared to those induced with β-estradiol (+ β-est). **B**) Root length of *ESR2:ER, ESR2:ER ipt5* and *ESR2:ER ahp6* seedlings 13 days after direct germination either in mock or ESR2 induction medium. One-way ANOVA test, followed by Fisher LSD post-hoc analysis, n = 18 to 37 plants, p-value ≤ 0.0001. Error bars represent SE. Different letters indicate different statistical groups. **C)** Development of induced *ESR2:ER, ESR2:ER ip5* and *ESR2:ER ahp6* plants 40 DAG. **D)** Vascular tissue in primary roots of induced *ESR2:ER, ESR2:ER ipt5* and *ESR2:ER ahp6* seedlings 15 days after induction, stained with basic fuchsin. Scale bars A) 6 DAG seedlings 0.3 mm, 17 DAG, 2 mm, C) 1 cm, D) 0.02 mm.

Figure 4. Effect of exogenous cytokinin treatment in callus development in *ESR2:ER ipt5* and *ESR2:ER ahp6* seedlings and root explants. A) Seedlings grown in medium supplemented with 20 μM β-estradiol and transplanted at 6 DAG to media with 30 μM 6-benzylaminopurine (BAP) and 20 μM β-estradiol, observed after 34 days after transference. A black arrowhead indicates a shoot-like structure in the hypocotyl-root junction. **B)** Seedlings directly germinated in medium supplemented with 30 μM 6-benzylaminopurine (BAP) and 20 μM β-estradiol, observed at 40 DAG. **C)** Wild type, *ESR2:ER, ahp6,* and *ESR2:ER ahp6* root explants transplanted at 7 DAG to Shoot Inducing Medium (SIM) supplemented with 20 μM β-estradiol (magnified view of the *ESR2:ER ahp6* explant is shown next to it, at the right side), and **D)** Wild type and *drnl-2* root explants in SIM (left) and their corresponding magnified views (right), observed 20 days after transference. Scale bars: A) shoots (top) 0.5 mm and roots (bottom) 0.2 mm; B) WT, *ESR2:ER,* and *ahp6-1* 0.5 mm*; ESR2:ER ahp6* and *ESR2:ER ipt5* 1 mm. C and D) 1 mm.

Figure 5. ESR2 regulation of *IPT5* and *AHP6* expression and similarity with *ESR2* expression. A) Schemes of *IPT5* and *AHP6* genomic regions tested by Y1H (*IPT5* complete (I) to III, *AHP6* I to V fragments) and NanoLuc assays (purple and yellow regions). Diamonds indicate GCC sites before the ATG of each gene (pink) or after (purple). Red crosses indicate fragments that showed autoactivation in the Y1H assays. **B)** Y1H assays for ESR2 protein interaction with *IPT5* and *AHP6* fragments. **C)** NanoLuc assays, the diagrams show the constructs used as

effector and reporters. The relative NanoLuc activity detected as bioluminescence (Relative Luminiscence Units, RLU) in each combination is presented in the graph. Values are given as mean ± SE, n = 4. Significant differences are indicated by asterisks (***p <0.001 in Student´s t-test). **D)** *ESR2* expression compared to *IPT5* and *AHP6* expression in aerial tissues of seedlings. From left to right, the first two microphotographs show longitudinal sections of *ESR2::GUS* and *IPT5::GUS* seedlings. Microphotographs in the middle show transversal sections of *ESR2::GUS* and *IPT5::GUS* seedlings. The last microphotographs show *ESR2::ESR2:GFP* and *AHP6::GFP* expression in young leaf primordia. In the GUS images, white arrowheads indicate stipules and in GFP images they indicate expression near the tip of the primordium in both cases (possibly associated to vascular tissue formation). Dashed lines delineate leaf primordia. Scale bars: 50 µm in GUS histological sections and 20 µm in GFP micrographs.

Figure 6. ESR2 regulation of genes involved in the cytokinin pathway and hypothetical model of action leading to root reprogramming and green callus formation. A) Callus formation and other phenotypes promoted by the induction of ESR2 activity depend on its modulation of the cytokinin (CK) pathway, both positively and negatively. Other ESR2-regulated genes (related to cytokinin or other processes) are also involved. **B)** Cytokinin genes regulated by ESR2 and their effect in the cytokinin pathway. The genes described by Zhang et al 2018, Jasinski et al., 2005, Yanai et al., 2005, Dai et al, 2023, Frerichs et al. 2019; Ikeda et al., 2006 and in this work are depicted. The genes in bold were studied in this work, and when mutated, abolish or severely reduce ESR2-promoted callus formation. **C)** Proposed hypothetical model of a possible scenario to explain the effect of ESR2 in cytokinin biosynthesis and inhibition of cytokinin signaling, creating regions or "fields" where cytokinins are produced but signaling is reduced, and regions to where cytokinins diffuse and signaling is not inhibited, eliciting a response. These putative differential cytokinin sensing "fields" could trigger the reprogramming of root cells to form green calli. Black and color arrows indicate the regulation studied in this work. Gray arrows indicate regulation described elsewhere. Arrows indicate positive regulation, and those ending in a perpendicular line instead of an arrowhead indicate negative regulation. Light blue block arrows represent cytokinin movement from a cell or region, to surrounding cells or regions. Green-colored areas indicate positive action, and violet-purple regions negative action upon the CK pathway.

References

Atta, R. *et al.* (2009). 'Pluripotency of Arabidopsis xylem pericycle underlies shoot regeneration from root and hypocotyl explants grown in vitro.' *Plant Journal*, *57*(4), pp. 626–644. https://doi.org/10.1111/j.1365-313X.2008.03715.x

Banno, H. *et al.* (2001). 'Overexpression of Arabidopsis ESR1 induces initiation of Shoot Regeneration.' *Plant Cell*, *13*(12), pp. 2609–2618. https://doi.org/10.1105/tpc.13.12.2609

Becerra-García, R. E., *et al.* (2023). 'A NanoLuc-Based Transactivation Assay in Plants.' *Methods in Molecular Biology (Clifton, N.J.)*, *2686*, pp. 553–565. https://doi.org/10.1007/978-1-0716-3299-4_26

Besnard, F. *et al.* (2014). 'Cytokinin signalling inhibitory fields provide robustness to phyllotaxis.' *Nature*, *505*(7483), pp. 417–421. https://doi.org/10.1038/nature12791

Bustillo-Avendaño, E. *et al.* (2018). 'Regulation of hormonal control, cell reprogramming, and patterning during de novo root organogenesis.' *Plant Physiology*, *176*(2), pp. 1709–1727. https://doi.org/10.1104/pp.17.00980

Capua, Y., and Eshed, Y. (2017). 'Coordination of auxin-triggered leaf initiation by tomato LEAFLESS.' *Proceedings of the National Academy of Sciences of the United States of America*, *114*(12), pp. 3246–3251. https://doi.org/10.1073/pnas.1617146114

Chandler, J. W. *et al.* (2011). 'DORNRÖSCHEN-LIKE expression marks Arabidopsis floral organ founder cells and precedes auxin response maxima.' *Plant Molecular Biology*, *76*(1–2), pp. 171–185. https://doi.org/10.1007/s11103-011-9779-8

Chandler, J. W., and Werr, W. (2014). 'Arabidopsis floral phytomer development: auxin response relative to biphasic modes of organ initiation.' *Journal of Experimental Botany*, *65*(12), pp. 3097–3110. https://doi.org/10.1093/JXB/ERU153

Chang, L., Ramireddy, E., and Schmülling, T. (2015). 'Cytokinin as a positional cue regulating lateral root spacing in Arabidopsis.' *Journal of Experimental Botany*, *66*(15), pp. 4759. https://doi.org/10.1093/JXB/ERV252

Che, P., Lall, S. and Howell, S.H. (2007). 'Developmental steps in acquiring competence for shoot development in *Arabidopsis* tissue culture.' *Planta*, *226*, pp. 1183–1194. https://doi.org/10.1007/s00425-007-0565-4

Chow, C. N. *et al.* (2019). 'PlantPAN3.0: a new and updated resource for reconstructing transcriptional regulatory networks from ChIP-seq experiments in plants.' *Nucleic Acids Research*, *47*(D1), pp. D1155–D1163. https://doi.org/10.1093/NAR/GKY1081

Cortleven, A., and Schmülling, T. (2015). 'Regulation of chloroplast development and function by cytokinin.' *Journal of Experimental Botany*, *66*(16), pp. 4999–5013. https://doi.org/10.1093/JXB/ERV132

Curtis, M. D., and Grossniklaus, U. (2003). 'A gateway cloning vector set for high-throughput functional analysis of genes in planta.' *Plant Physiology*, *133*(2), pp. 462–469. https://doi.org/10.1104/PP.103.027979

Dai, Y., Luo, L., and Zhao, Z. (2023). 'Genetic robustness control of auxin output in priming organ initiation.' *Proceedings of the National Academy of Sciences of the United States of America*, *120*(28). https://doi.org/10.1073/PNAS.2221606120

De Rybel, B. *et al.* (2016). 'Plant vascular development: from early specification to differentiation.' *Nat Rev Mol Cell Biol* **17**, pp. 30–40. https://doi.org/10.1038/nrm.2015.6

Dello Ioio, R. *et al.* (2007). 'Cytokinins Determine Arabidopsis Root-Meristem Size by Controlling Cell Differentiation.' *Current Biology*, *17*(8), pp. 678–682. https://doi.org/10.1016/j.cub.2007.02.047

Dello Ioio, R. *et al.* (2008). 'A genetic framework for the control of cell division and differentiation in the root meristem.' *Science (New York, N.Y.)*, *322*(5906), pp. 1380–1384. https://doi.org/10.1126/SCIENCE.1164147

Durán-Medina, Y. *et al.* (2017a). 'The AP2/ERF transcription factor DRNL modulates gynoecium development and affects its response to Cytokinin.' *Frontiers in Plant Science*, *8*, 298950. https://doi.org/10.3389/FPLS.2017.01841/BIBTEX

Durán-Medina, Y., Díaz-Ramírez, D., and Marsch-Martínez, N. (2017b). 'Cytokinins on the move.' *Frontiers in Plant Science*, *8*(FEBRUARY), 236657. https://doi.org/10.3389/FPLS.2017.00146/BIBTEX

Efferth, T. (2019). 'Biotechnology Applications of Plant Callus Cultures.' *Engineering* 5 *(1)*, pp. 50-59. https://doi.org/10.1016/j.eng.2018.11.006

Eklund, D. M. *et al.* (2011a). 'Expression of arabidopsis SHORT INTERNODES/ STYLISH family genes in auxin biosynthesis zones of aerial organs is dependent on a GCC box-like regulatory element.' *Plant Physiology*, *157*(4), pp. 2069–2080. https://doi.org/10.1104/pp.111.182253

Frerichs, A. *et al.* (2019). 'Specific chromatin changes mark lateral organ founder cells in the Arabidopsis inflorescence meristem.' *Journal of Experimental Botany*, *70*(15), pp. 3867–3879. https://doi.org/10.1093/jxb/erz181

Fujimoto, S. Y. *et al.* (2000). 'Arabidopsis ethylene-responsive element binding factors act as transcriptional activators or repressors of GCC box-mediated gene expression.' *Plant Cell*, *12*(3), pp. 393–404. https://doi.org/10.1105/tpc.12.3.393

Glowa, D. *et al.* (2021). 'Clonal sector analysis and cell ablation confirm a function for DORNROESCHEN-LIKE in founder cells and the vasculature in Arabidopsis.' *Planta*, *253*(2), pp. 27. https://doi.org/10.1007/S00425-020-03545-5

Gordon, S.P. *et al.* (2007). 'Pattern formation during de novo assembly of the *Arabidopsis* shoot meristem.' *Development* 134*(19)*, pp. 3539–3548. https://doi: https://doi.org/10.1242/dev.010298

Hao, D., Ohme-Takagi, M., and Sarai, A. (1998). 'Unique mode of GCC box recognition by the DNA-binding domain of ethylene-responsive element-binding factor (ERF domain) in plant.' *The Journal of Biological Chemistry*, *273*(41), pp. 26857–26861. https://doi.org/10.1074/JBC.273.41.26857

Ibáñez, S. *et al.* (2020). 'Advances in Plant Regeneration: Shake, Rattle and Roll.' *Plants, 9 (7)* pp. *897,* https://doi.org/10.3390/PLANTS9070897

Ikeda, Y. *et al.* (2006a). 'The ENHANCER OF SHOOT REGENERATION 2 Gene in Arabidopsis Regulates CUP-SHAPED COTYLEDON 1 at the Transcriptional Level and Controls Cotyledon

Development.' *Plant & Cell Physiology*, *47*(11), pp. 1443–1456. https://doi.org/10.1093/PCP/PCL023

Ikeuchi, M. *et al.* (2019). 'Molecular Mechanisms of Plant Regeneration.' *Annual Review of Plant Biology*, *70*(1), pp. 377–406. https://doi.org/10.1146/annurev-arplant-050718-100434

Ikeuchi, M. *et al.* (2016). 'Plant regeneration: Cellular origins and molecular mechanisms.' *Development (Cambridge)* 143(9) pp. 1442–1451). https://doi.org/10.1242/dev.134668

Ikeuchi, M., Sugimoto, K., and Iwase, A. (2013). 'Plant callus: Mechanisms of induction and repression.' *Plant Cell,* 25(9) pp. 3159–3173. https://doi.org/10.1105/tpc.113.116053

Jasinski, S. *et al.* (2005). 'KNOX Action in Arabidopsis Is Mediated by Coordinate Regulation of Cytokinin and Gibberellin Activities.' *Current Biology*, *15*(17), pp. 1560–1565. https://doi.org/10.1016/J.CUB.2005.07.023

Kakimoto, T. (2001). 'Identification of Plant Cytokinin Biosynthetic Enzymes as Dimethylallyl Diphosphate: ATP/ADP Isopentenyltransferases.' *Plant and Cell Physiology*, *42*(7), pp. 677–685. https://doi.org/10.1093/PCP/PCE112

Kirch, T. *et al.* (2003). 'The DORNRÖSCHEN/ENHANCER OF SHOOT REGENERATION 1 gene of Arabidopsis acts in the control of meristem cell fate and lateral organ development.' *Plant Cell*, *15*(3), pp. 694–705. https://doi.org/10.1105/tpc.009480

Köllmer, I. *et al.* (2014). 'Overexpression of the cytosolic cytokinin oxidase/dehydrogenase (CKX7) from Arabidopsis causes specific changes in root growth and xylem differentiation.' *The Plant Journal*, *78*(3), pp. 359–371. https://doi.org/10.1111/TPJ.12477

Laplaze, L. *et al.* (2005). 'GAL4-GFP enhancer trap lines for genetic manipulation of lateral root development in *Arabidopsis thaliana*.' *Journal of Experimental Botany*, *56*(419), pp. 2433–2442, https://doi.org/10.1093/jxb/eri236

Liu, C. J., Zhao, Y., and Zhang, K. (2019). 'Cytokinin transporters: Multisite players in cytokinin homeostasis and signal distribution.' *Frontiers in Plant Science*, *10*, pp. 449767. https://doi.org/10.3389/FPLS.2019.00693/BIBTEX

Liu, S. *et al.* (2022). 'Cytokinin promotes growth cessation in the Arabidopsis root.' *Current Biology*, *32*(9), pp. 1974-1985.e3. https://doi.org/10.1016/J.CUB.2022.03.019

Mähönen, A. P. *et al.* (2006). 'Cytokinin signaling and its inhibitor AHP6 regulate cell fate during vascular development.' *Science*, *311*(5757), pp. 94–98. https://doi.org/10.1126/science.1118875

Mähönen, A. P. *et al.* (2000). 'A novel two-component hybrid molecule regulates vascular morphogenesis of the Arabidopsis root.' *Genes and Development*, *14*(23), pp. 2938–2943. https://doi.org/10.1101/gad.189200

Marsch-Martinez, N. *et al.* (2006). 'BOLITA, an Arabidopsis AP2/ERF-like transcription factor that affects cell expansion and proliferation/differentiation pathways.' *Plant Molecular Biology*, *62*(6), pp. 825–843. https://doi.org/10.1007/S11103-006-9059-1/METRICS

Matsumoto-Kitano, M. *et al.* (2008). 'Cytokinins are central regulators of cambial activity.' *Proceedings of the National Academy of Sciences of the United States of America*, *105*(50), pp. 20027–20031. https://doi.org/10.1073/pnas.0805619105

Matsuo, N., Makino, M., and Banno, H. (2011). 'Arabidopsis ENHANCER OF SHOOT REGENERATION (ESR)1 and ESR2 regulate in vitro shoot regeneration, and their expressions are differentially regulated.' *Plant Science*, *181*(1), pp. 39-46. https://doi.org/10.1016/j.plantsci.2011.03.007

Melnyk, C. W. (2023). 'Quantitative regeneration: Skoog and Miller revisited.' *Quantitative Plant Biology*, *4*. https://doi.org/10.1017/QPB.2023.9

Miyawaki, K., Matsumoto-Kitano, M., and Kakimoto, T. (2004). 'Expression of cytokinin biosynthetic isopentenyltransferase genes in Arabidopsis: Tissue specificity and regulation by auxin, cytokinin, and nitrate.' *Plant Journal*, *37*(1), pp. 128–138. https://doi.org/10.1046/j.1365-313X.2003.01945.x

Miyawaki, K. *et al.* (2006). 'Roles of *Arabidopsis* ATP/ADP isopentenyltransferases and tRNA isopentenyltransferases in cytokinin biosynthesis.' *Proceedings of the National Academy of Sciences*, *103*(44), pp. 16598–16603. https://doi.org/10.1073/pnas.0603522103

Müller, C. J. *et al.* (2017). 'Cytokinin-Auxin Crosstalk in the Gynoecial Primordium Ensures Correct Domain Patterning.' *Plant Physiology*, *175*(3), pp. 1144–1157. https://doi.org/10.1104/PP.17.00805

Murashige, T., and Skoog, F. (1962). 'A Revised Medium for Rapid Growth and Bioassays with Tobacco Tissue Cultures.' *Physiologia Plantarum*, *15*(3), pp. 473–497. https://doi.org/10.1111/j.1399-3054.1962.tb08052.x

Nag, A., Yang, Y., and Jack, T. (2007). 'DORNROSCHEN-LIKE, an AP2 gene, is necessary for stamen emergence in Arabidopsis.' *Plant Molecular Biology*, *65*(3), pp. 219–232. https://doi.org/10.1007/S11103-007-9210-7

Nedvěd, D. *et al.* (2021). 'Differential subcellular distribution of cytokinins: How does membrane transport fit into the big picture?' *International Journal of Molecular Sciences*, *22*(7), pp. 3428. https://doi.org/10.3390/IJMS22073428/S1

Ohashi-Ito, K. *et al.* (2014). 'A bHLH complex activates vascular cell division via cytokinin action in root apical meristem.' *Current Biology*, *24*(17), pp. 2053–2058. https://doi.org/10.1016/j.cub.2014.07.050

Ohme-Takagi, M., and Shinshi, S. (1995). 'Ethylene-inducible DNA binding proteins that interact with an ethylene-responsive element.' *The Plant Cell*, *7*(2), pp. 173–182. https://doi.org/10.1105/TPC.7.2.173

Oppenheimer, D. G. *et al.* (1991). 'A myb gene required for leaf trichome differentiation in Arabidopsis is expressed in stipules.' *Cell*, *67*(3), pp. 483–493. https://doi.org/10.1016/0092-8674(91)90523-2

Pernisova, M. *et al.* (2018). 'Cytokinin signalling regulates organ identity via the AHK4 receptor in arabidopsis.' *Development (Cambridge)*, *145*(14). https://doi.org/10.1242/dev.163907

Sakai, H. *et al.* (2001). 'ARR1, a transcription factor for genes immediately responsive to cytokinins.' *Science*, *294*(5546), pp. 1519–1521. https://doi.org/10.1126/SCIENCE.1065201/ASSET/97CCD9AC-635B-4776-B446-EC28EBE341B9/ASSETS/GRAPHIC/SE4519939004.JPEG

Shin, J., Bae, S., and Seo, P.J. (2020) '*De novo* shoot organogenesis during plant regeneration,' *Journal of Experimental Botany*, *71*(1), pp. 63–72. https://doi.org/10.1093/jxb/erz395

Skoog, F., and Miller, C. O. (1957). 'Chemical regulation of growth and organ formation in plant tissues cultured in vitro.' *Symposia of the Society for Experimental Biology*, *11*, pp. 118–130.

Šmeringai, J., Schrumpfová, P. P., and Pernisová, M. (2023). 'Cytokinins – regulators of de novo shoot organogenesis.' *Frontiers in Plant Science*, *14*, pp. 1239133. https://doi.org/10.3389/FPLS.2023.1239133/BIBTEX

Sohlberg, J. J. *et al.* (2006). 'STY1 regulates auxin homeostasis and affects apical–basal patterning of the Arabidopsis gynoecium.' *The Plant Journal*, *47*(1), pp. 112–123. https://doi.org/10.1111/J.1365-313X.2006.02775.X

Song, X. *et al.* (2023). 'Spatial transcriptomics reveals light-induced chlorenchyma cells involved in promoting shoot regeneration in tomato callus.' *Proceedings of the National Academy of Sciences U.S.A*, 120*(38)*, e2310163120. https://doi.org/10.1073/pnas.2310163120 (2023)

Sotelo-Silveira, M. *et al.* (2013). 'Cytochrome P450 CYP78A9 Is Involved in Arabidopsis Reproductive Development.' *Plant Physiology*, 162*(2)*, pp. 779–799. https://doi.org/10.1104/pp.113.218214

Sugimoto, K., Jiao, Y. and Meyerowitz, E.M. (2010). 'Arabidopsis regeneration from multiple tissues occurs via a root development pathway.' *Developmental Cell, 18*(3), pp. 463-471. https://doi.org/10.1016/j.devcel.2010.02.004.

Sun, J. *et al.* (2003). 'The Arabidopsis AtIPT8/PGA22 gene encodes an Isopentenyl Transferase that is involved in de *novo* cytokinin biosynthesis.' *Plant Physiology*, *131*(1), pp. 167. https://doi.org/10.1104/PP.011494

Svačinová, J. *et al.* (2012). 'A new approach for cytokinin isolation from Arabidopsis tissues using miniaturized purification: pipette tip solid-phase extraction.' *Plant Methods*, *8*(1), pp. 17–17. https://doi.org/10.1186/1746-4811-8-17

Urquiza-García, U., and Millar, A. J. (2019). 'Expanding the bioluminescent reporter toolkit for plant science with NanoLUC.' *Plant Methods*, *15*(1). https://doi.org/10.1186/S13007-019-0454-4

Ward, J. M. *et al.* (2006). 'A new role for the Arabidopsis AP2 Transcription Factor, LEAFY PETIOLE, in Gibberellin-induced germination is revealed by the misexpression of a homologous gene, SOB2/DRN-LIKE.' *The Plant Cell*, *18*(1), pp. 29. https://doi.org/10.1105/TPC.105.036707

Werner, T. *et al.* (2003). 'Cytokinin-deficient transgenic arabidopsis plants show multiple developmental alterations indicating opposite functions of cytokinins in the regulation of shoot and root meristem activity.' *The Plant Cell*, *15*(11), pp. 2532–2550. https://doi.org/10.1105/TPC.014928

Yanai, O. *et al.* (2005). 'Arabidopsis KNOXI proteins activate cytokinin biosynthesis.' *Current Biology*, *15*(17), pp. 1566–1571. https://doi.org/10.1016/j.cub.2005.07.060

Yang, B. J. *et al.* (2021). 'Non-cell autonomous and spatiotemporal signalling from a tissue organizer orchestrates root vascular development.' *Nature Plants*, *7*(11), pp. 1485–1494. https://doi.org/10.1038/S41477-021-01017-6

Ye, L. *et al.* (2021). 'Cytokinins initiate secondary growth in the Arabidopsis root through a set of LBD genes.' *Current Biology*, *31*(15), pp. 3365. https://doi.org/10.1016/J.CUB.2021.05.036

Zhang, C. *et al.* (2018). 'Spatiotemporal control of axillary meristem formation by interacting transcriptional regulators.' *Development (Cambridge)*, *145*(24). https://doi.org/10.1242/dev.158352

Zubko, E. *et al.* (2002). 'Activation tagging identifies a gene from Petunia hybrida responsible for the production of active cytokinins in plants.' *The Plant Journal*, *29*(6), pp. 797–808. https://doi.org/10.1046/J.1365-313X.2002.01256.X

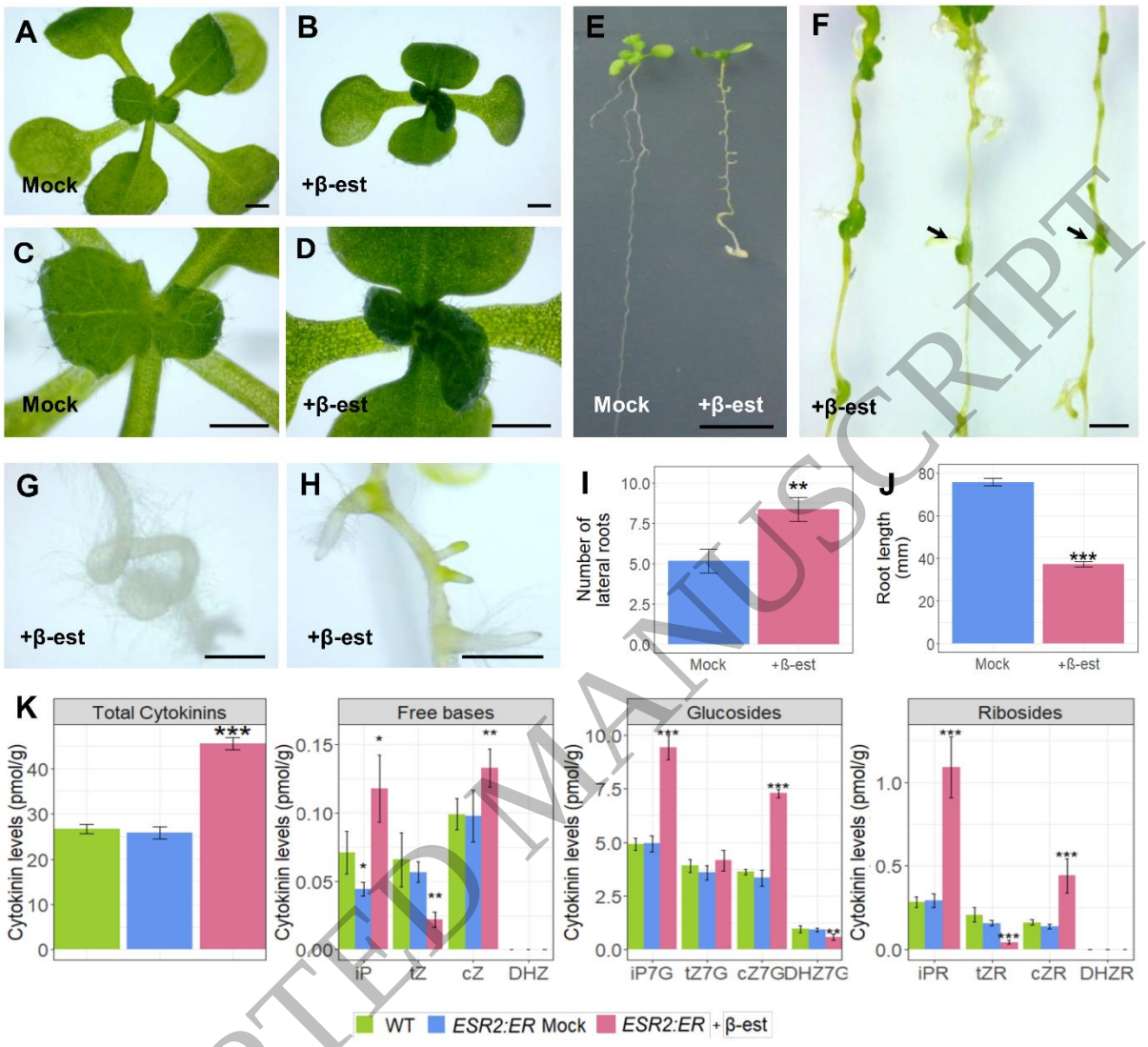

Figure 1
165x147 mm (x DPI)

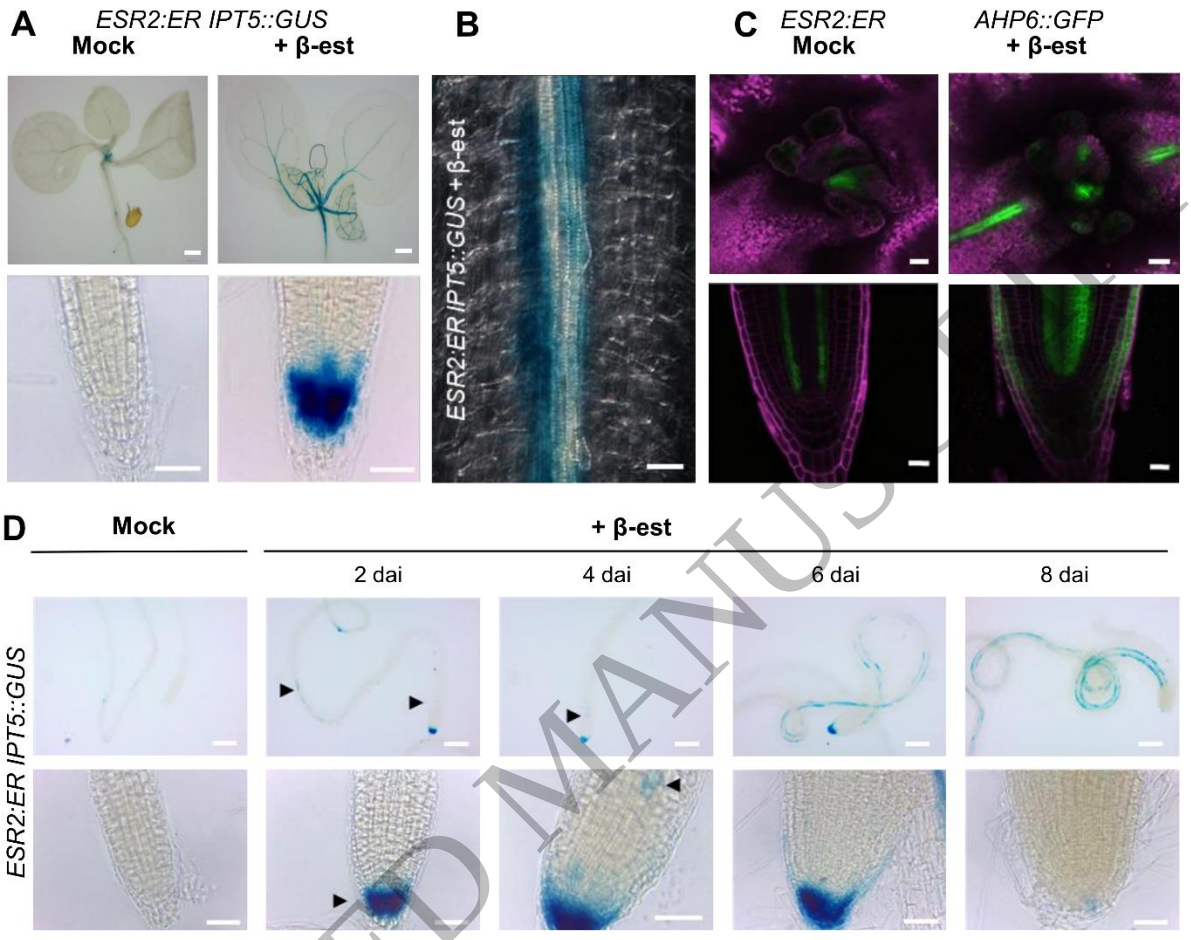

Figure 2
165x138 mm (x DPI)

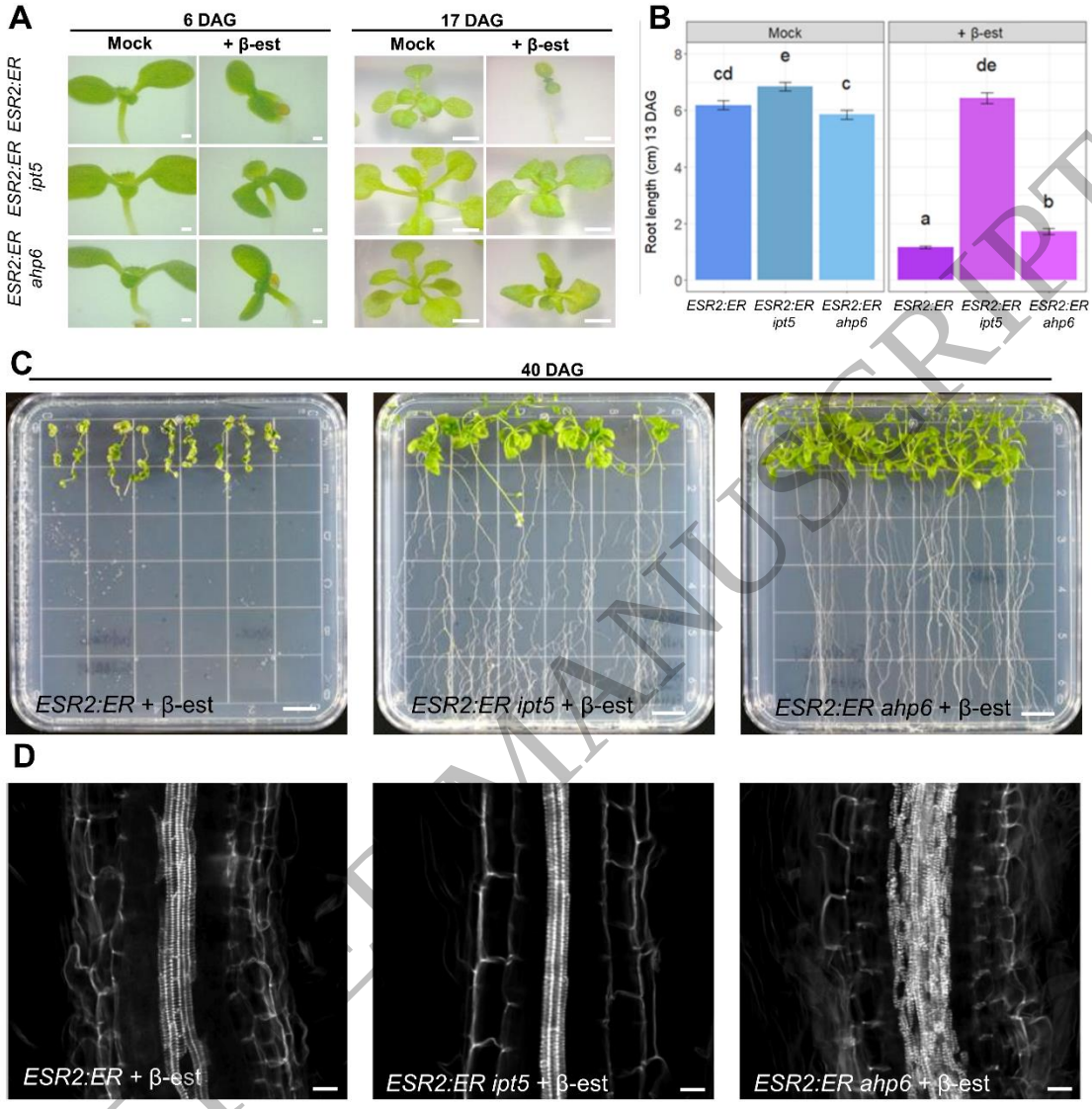

Figure 3
165x159 mm (x DPI)

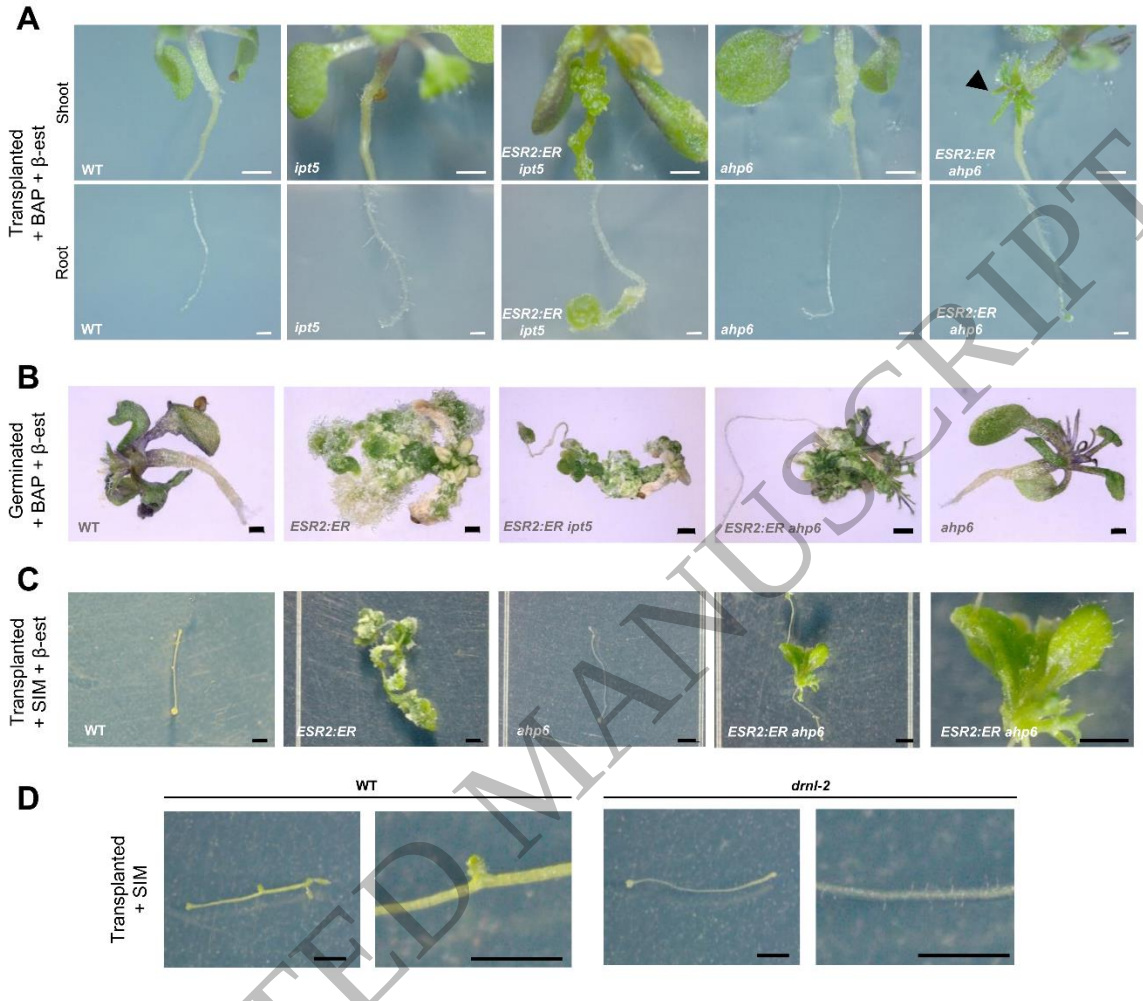

Figure 4
165x147 mm (x DPI)

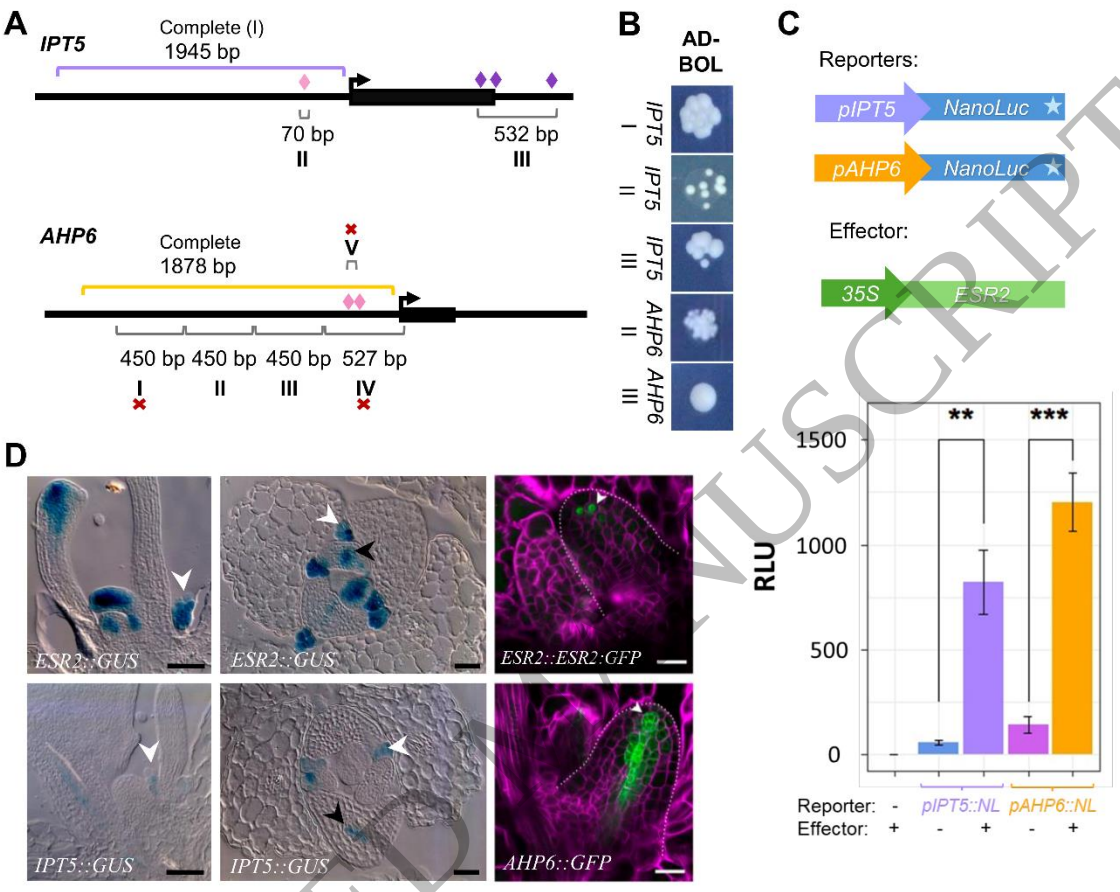

Figure 5
165x139 mm (x DPI)

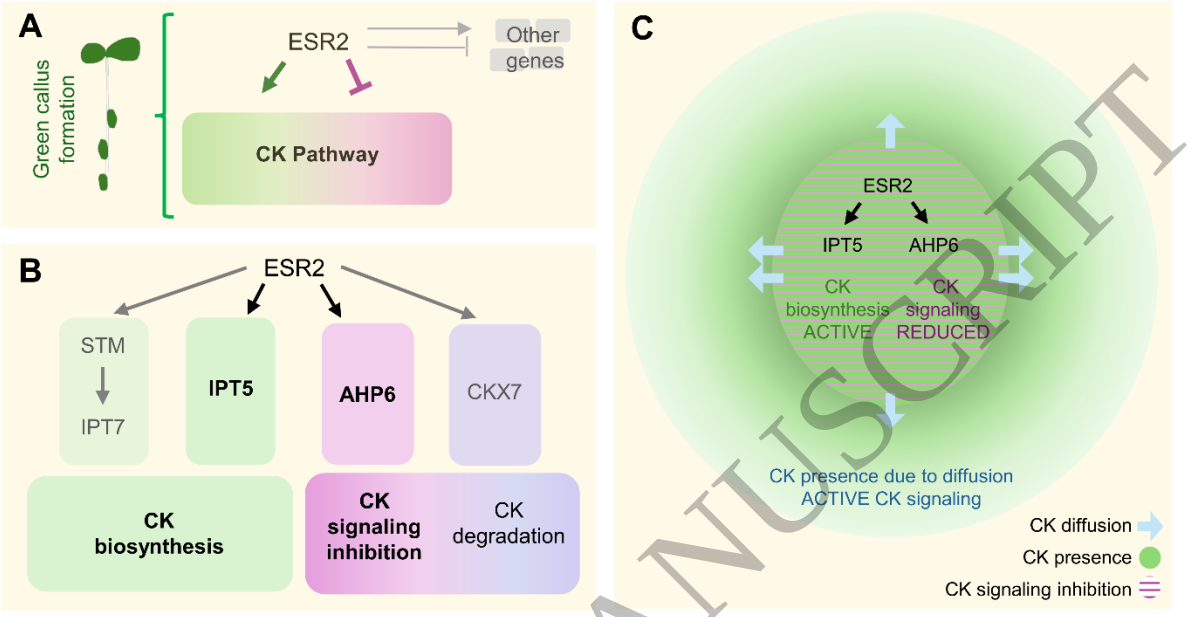

Figure 6
165x113 mm (x DPI)